NON-CONSERVATIVE DYNAMICS OF SPINNING BEAM SYSTEMS WITH GENERAL BOUNDARY CONDITIONS

by

JOHN A. PLAXTON

A Thesis
Submitted to the Faculty of Graduate Studies
in Partial fulfillment of the Requirements
for the Degree of

MASTER OF SCIENCE

Department of Mechanical and Industrial Engineering
University of Manitoba
Winnipeg, Manitoba, Canada

December 5, 1995

NON-CONSERVATIVE DYNAMICS OF SPINNING BEAM SYSTEMS WITH GENERAL BOUNDARY CONDITIONS

BY

JOHN. A. PLAXTON

A Thesis submitted to the Faculty of Graduate Studies of the University of Manitoba in partial fulfillment of the requirements of the degree of

MASTER OF SCIENCE

I hereby declare that I am the sole author of this thesis.

I authorize the University of Manitoba to lend this thesis to other institutions or individuals for the purpose of scholarly research.

I further authorize the University of Manitoba to reproduce this thesis by photocopying or by other means, in total or in part, at the request of other institutions or individuals for the purpose of scholarly research.

Abstract

This thesis uses analytical techniques to solve for the free and forced vibration response of non-conservative, spinning Timoshenko beams. The free vibration analytical method employs differential matrix operators and an appropriately defined state vector to reduce the partial differential equations to a system of ordinary differential equations. A series-type solution is used to solve the system of ordinary differential equations. The forced vibration analytical method requires an analysis of the adjoint system since the presence of distributed follower forces destroy physical symmetry, hence, making the problem non-self adjoint. The adjoint analysis yields eigenvalues and eigenvectors of the adjoint of the problem. Modal expansion over the real and adjoint system eigenvectors is used to determine the dynamic response of non-conservative, spinning Timoshenko beams.

The free vibration analysis is performed for six boundary condition cases. Each case is investigated for the influence of beam spin rate and magnitude of follower force upon the natural frequencies of the beams. Both the forward and backward precession frequencies are investigated. The forced vibration analysis is performed for the four boundary condition cases that do not include rigid body motion. Results are presented showing the response of each of the boundary condition cases to an exponentially decreasing transverse load for various follower force loadings.

Acknowledgments

I would like to express my appreciation to my advisor Dr. Ray Han and also, Dr. Jean Wu-Zheng Zu for their guidance and support. I would like to express my thanks to the Natural Sciences and Engineering Research Council (NSERC) for its financial support during the first two years of my thesis. I would also like to extend appreciation to my present employer, Elsag Bailey (Canada) Inc., for affording me the time to finish my thesis.

Finally, I wish to express my gratitude to my fiancé and parents for the understanding and support during the past three years.

Contents

List of Tables

List of Figures

Chapter 1

Introduction

Problem Definition

Spinning beam systems form the foundation of numerous engineering applications found in the physical world today. Rocket and other flight vehicles, rotating workpieces in machining operations, and turbine engines in rotordynamic systems are examples of physical systems developed from spinning beam systems. Research into this field has been the focus of researchers since the late 1800's. However, over the last few decades, the complexity of this research has grown significantly, and this is not only due to the fact that engineering systems have become increasingly sophisticated, but is also due to the availability of cheap and powerful computers to handle their analyses.

The majority of research to date has been based upon the Euler-Bernoulli beam theory. Also known as the simple beam theory, this beam theory has limits beyond which the application of the model is inappropriate. The simple beam theory is valid only for slender beams, and also, only for the first couple of modes of vibration. For higher modes vibration applications, the simple beam theory introduces significant error, even for slender beams. For example, accurate modeling of the behavior prediction of high-speed spinning equipment is critical to obtain satisfactory bearing load predictions and, thus, machine performance.

The Timoshenko beam theory was born out of the need for a beam theory encompassing beam configurations that are short and thick. For such stubby structures,

the effects of shear deformation and rotary inertia cannot be neglected as was assumed in the case of the Euler-Bernoulli beam theory. By including these effects in the model, the Timoshenko beam theory can correctly predict the behavior of stubby beams. The theory is also capable of predicting higher order modes of vibration for both slender and stubby beams, with greater accuracy than is possible by the Euler-Bernoulli beam theory. However, the Timoshenko beam model does not come without a price. Unlike the Euler-Bernoulli beam theory which involves solving a single ordinary differential equation, the Timoshenko beam model is based on solving coupled partial differential equations. Partial differential equations are considerably more difficult to solve analytically and only a few possess such analytical solutions. Frequently these equations are solved numerically, and therefore, suffered from a lack of a closed-form solutions which can be very useful for the purpose of verification and bench-marking of the numerical results.

In this thesis, a method of analytically solving the Timoshenko beam model for spinning beams with general boundary conditions and subjected to distributed follower forces and arbitrary lateral loads is developed. The free and forced vibration characteristics of spinning Timoshenko beams are investigated.

Literature Survey

Since this thesis deals with the analytical solution of the Timoshenko beam model it is important to establish what has already been done in this field. An important aspect of the study is the evaluation of the stability of beam systems. A comprehensive study in this area can be found in the work of Bolotin (1963) and more recently in Huseyin (1978). Beal (1965) studied the stability of a uniform free-free Euler-Bernoulli beam under controlled concentrated follower forces. The use of the concept of adjointness in a follower force system was mentioned by Nemat-Nasser and Herrmann (1966). They attempted to offer a physical interpretation of the original and adjoint systems by associating them with an energy sink and an energy source respectively. Further

extensions to handle a follower-force system expressed as tangential end torques was presented by Nemat-Nasser (1968), and in the form of the follower-type surface tractions by Prasad and Herrmann (1969). The work described so far has been confined to stability analysis of non~self-adjoint problems due to the action of concentrated end follower forces. Leipholz and Madan (1975) investigated the stability of Euler-Bernoulli beams subjected to distributed follower forces. They solved the differential equations of motion in terms of Bessel solutions. Wu (1976a) also investigated the stability of free-free Euler-Bernoulli beams based on the Bessel solution method. For the case of free-free Euler-Bernoulli beams with a controlled axial force, Wu (1976b) proposed a finite element approach to study their stability. Park and Mote (1985) employed a finite element model of a uniform, free-free Euler-Bernoulli beam to investigate the dynamic effects caused by a concentrated follower force. The stability of the model was investigated with respect to axial location of the mass, location of follower force control sensor, sensor gain, and magnitude of force. Also, using a finite element model, Park (1987) investigated the stability of a free-free Timoshenko beam driven by a controlled concentrated follower force. In particular, he studied the influence of shear deformation and rotary inertia on the stability of stubby beams. Kounadis (1980) formulated the equations of motion for an elastically restrained Timoshenko beam carrying a concentrated mass and subjected to a compressive follower load and a distributed compressive follower load. He derived the equations using the principle of virtual work and Hamilton's principle for non-conservative systems, and compared with the results he obtained via a free body diagram approach (Newton method). He showed that while the results are consistent with those derived via Hamilton's principle for a non-conservative system, they do not agree with the equations based on the classical dynamic equilibrium approach. He did not however, attempt to solve any of the equations he obtained. Platus (1992) developed a Lagrangian formulation to derive the equations of motion for a spinning Euler-Bernoulli beam. He modeled a free-free beam with rigid-body motion. His investigation yielded results defining the stability of a free-free beam. Chen and Ku (1994) investigated the stability of a cantilevered column subjected to uniformly distributed in-plane follower forces. Their work was performed using a finite element method for Timoshenko beams. Kounadis

(1994) in his work on the divergence instability of non-conservative systems, argued that the validity of the various phenomena based on the classical linear undamped theory is questionable when a nonlinear model, including damping, is employed.

Mukhopahyay (1988) investigated the free vibration of a free-free Timoshenko beam using a flexibility matrix approach to remove the singularity caused by free-body motion. Rao and Rao (1989) presented the results of investigating large amplitude vibrations of tapered clamped-free and free-free beams. They modeled the beam using an Euler-Bernoulli beam model and solved using a fourth-order Runge-Kutta integration algorithm. Using a finite element technique, Leung (1988) obtained natural frequencies of a follower force system modeled by the Timoshenko beam element. Employing the Euler-Bernoulli beam theory, Craig and Ni (1989) investigated a model-order reduction method applied to a free-free beam.

Work on the dynamics of *spinning* beam systems has been limited. Bauer (1980) presented eigenvalues and eigenfunctions for rotating uniform beams. His solution was derived from the Euler-Bernoulli beam theory. He presented results for the six classical boundary conditions. Zu and Han (1992) investigated the natural frequencies and normal modes of a spinning Timoshenko beam with general boundary conditions. They presented analytical solutions for each of the six classical boundary conditions. Zu, Han and Lu (1995) investigated the critical speeds of a spinning Timoshenko beam. They presented precession frequencies and critical speeds for six classical boundary conditions. Han and Zu (1992, 1993) investigated the analytical dynamics of a spinning Timoshenko beam with a moving load. A simply supported beam was investigated. Eighth-order coupled differential equations describing the motion of the beam were reduced to a set of uncoupled fourth-order differential equations.

The field of the dynamic analysis of non~self-adjoint systems has been investigated mainly by Leipholz and his co-workers. Dynamic response computations were presented by Leipholz (1983) and also, by Afagh and Leipholz (1990), and response due to

transverse shock loads by Afagh and Lee (1991). Afagh and Leipholz (1990) used a Green's function approach to the solution of the dynamics of Euler-Bernoulli beams undergoing tangential distributed follower forces. Their method was applied to the solution of a clamped-free beam. All these studies are based on the Euler-Bernoulli beam theory. The dynamics of spinning Timoshenko beams with distributed follower forces has been overlooked by researchers for the most part. Zu, Han and Williams (1993) solved the free and forced vibration problem for a spinning Timoshenko beam with distributed follower forces. They applied an analytical solution based upon adjoint system analysis to the dynamics of a clamped-free beam.

Proposed Research

In this thesis, the analytical solution for the spinning Timoshenko beam with distributed follower forces presented by Zu (1993) will be expanded to include all the boundary conditions of interest in dynamics analysis. The free vibration characteristics will be determined for beams under the following boundary conditions: clamped-free, clamped-clamped, clamped-hinged, hinged-hinged, hinged-free, and free-free. The forced vibration analysis will be performed for four of the six boundary conditions: clamped-free, clamped-clamped, clamped-hinged, and hinged-hinged. The remaining two boundary conditions, hinged-free and free-free, are omitted. The hinged-free forced vibration case is of little engineering value is therefore omitted. The free-free case has the added complication of inertia coupling due to rigid-body motion, and is therefore left for future investigation. A limited stability analysis will be performed to assess the validity of critical distributed follower forces used for non-dimensionalization of parameters. From this analysis two different types of instability will be identified in the spinning beam systems.

Chapter 2

Free Vibration Analysis

Introduction

This chapter presents the free vibration analysis of a Timoshenko beam under the influence of distributed follower forces for six boundary condition cases: clamped-free, clamped-clamped, clamped-hinged, hinged-hinged, hinged-free, and free-free cases. The case of a clamped-free beam has been previously investigated by Zu, Han, and Williams (1993). Zu et al. employed analytical methods to determine the free vibration and forced vibration characteristics of a clamped-free Timoshenko beam. For the thesis, the work of Zu et al. has been extended to include the dynamics of the other five boundary condition cases mentioned earlier.

Formulation

The equations of motion for a spinning Timoshenko beam sketched in Figure 2.1, including uniformly distributed follower force q and lateral force p, have been derived previously by Zu et al. In complex notation, they are as follows:

$$\frac{\partial^2 u}{\partial t^2} + \frac{\kappa G}{\rho l^2}\left(l\frac{\partial \psi}{\partial \zeta} - \frac{\partial^2 u}{\partial \zeta^2}\right) + \frac{q(1-\zeta)}{\rho A l}\frac{\partial^2 u}{\partial \zeta^2} = \frac{p}{\rho A} \tag{2.1}$$

$$\frac{\partial^2 \psi}{\partial t^2} - i\frac{\Omega J_z}{\rho I}\frac{\partial \psi}{\partial t} - \frac{E}{\rho l^2}\frac{\partial^2 \psi}{\partial \zeta^2} + \frac{\kappa A G}{\rho I l}\left(l\psi - \frac{\partial u}{\partial \zeta}\right) = 0 \tag{2.2}$$

where ρ, l, A, I, J_z, E, G and κ are the mass density, length, cross-sectional area, transverse moment of inertia of an axisymmetric cross-section, polar mass moment of inertia, Young's modulus, shear modulus and shear coefficient of the beam, respectively, and $i = \sqrt{-1}$. The variable u is defined to be the complex variable of transverse deflection, and ψ is defined to be the complex variable of bending angle.

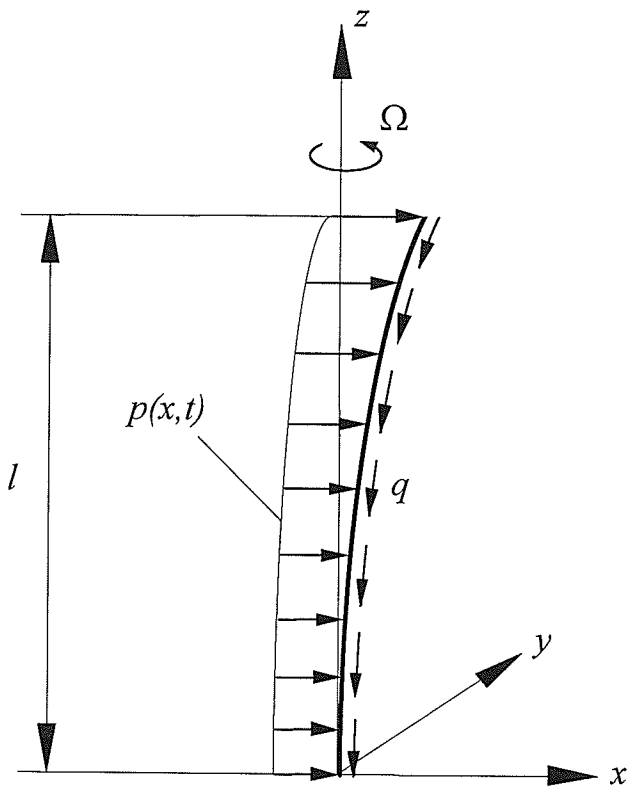

Figure 2.1: A Spinning Beam System

Three of the possible end conditions that can be applied to the system are the clamped, hinged, and free boundary conditions. The end conditions required by each case are:

Clamped:

$$u(\zeta,t) = 0$$
$$\psi(\zeta,t) = 0$$

Hinged:

$$u(\zeta,t) = 0$$
$$\psi'(\zeta,t) = 0$$

Free:

$$\psi'(\zeta,t)=0$$
$$\frac{u'(\zeta,t)}{l}-\psi(\zeta,t)=0$$

where $\zeta=0$ or 1 and $(\,)'$ implies $\partial(\,)/\partial\zeta$. A time transformation, $\tau=it$, is applied to remove the complex term in equation (2.2). The equations of motion now become:

$$-\frac{\partial^2 u}{\partial\tau^2}+\frac{\kappa G}{\rho l^2}\left(l\frac{\partial\psi}{\partial\zeta}-\frac{\partial^2 u}{\partial\zeta^2}\right)+\frac{q(1-\zeta)}{\rho A l}\frac{\partial^2 u}{\partial\zeta^2}=\frac{p}{\rho A} \tag{2.3}$$

$$-\frac{\partial^2\psi}{\partial\tau^2}+\frac{\Omega J_z}{\rho I}\frac{\partial\psi}{\partial\tau}-\frac{E}{\rho l^2}\frac{\partial^2\psi}{\partial\zeta^2}+\frac{\kappa AG}{\rho I l}\left(l\psi-\frac{\partial u}{\partial\zeta}\right)=0 \tag{2.4}$$

The equations of motion can be expressed in matrix form as follows:

$$[M]\{\dot{w}\}=[K]\{w\}+\{P\} \tag{2.5}$$

where $\dot{(\,)}$ implies $\partial(\,)/\partial\tau$ and $\{w\}$ is the state vector defined as follows:

$$\{w\}=\langle\dot{u}\;\; u\;\; \dot{\psi}\;\; \psi\rangle^T \tag{2.6}$$

$[M]$ and $[K]$ are differential matrix operators representing generalized mass and stiffness matrices, and $\{P\}$ a load vector. They are given by:

$$[M]=\begin{bmatrix}0 & A/I & 0 & 0\\ A/I & 0 & 0 & 0\\ 0 & 0 & 0 & 1\\ 0 & 0 & 1 & -\Omega\dfrac{J_z}{\rho I}\end{bmatrix} \tag{2.7}$$

$$[K]=\begin{bmatrix}A/I & 0 & 0 & 0\\ 0 & \left(-\dfrac{\kappa AG}{\rho I l^2}+\dfrac{q(1-\zeta)}{\rho I l}\right)\dfrac{\partial^2}{\partial\zeta^2} & 0 & \dfrac{\kappa AG}{\rho I l}\dfrac{\partial}{\partial\zeta}\\ 0 & 0 & 1 & 0\\ 0 & -\dfrac{\kappa AG}{\rho I l}\dfrac{\partial}{\partial\zeta} & 0 & -\dfrac{E}{\rho l^2}\dfrac{\partial^2}{\partial\zeta^2}+\dfrac{\kappa AG}{\rho I}\end{bmatrix} \tag{2.8}$$

$$\{P\} = \left\langle 0 \quad \frac{p}{\rho I} \quad 0 \quad 0 \right\rangle^T \tag{2.9}$$

For free vibration analysis, $\{P\}$ is set to zero and the eigenproblem to be solved is

$$\lambda_m [M]\{W\}_m = [K]\{W\}_m \qquad m = \pm 1, \pm 2, \ldots \tag{2.10}$$

where λ_m is the eigenvalue of the system. Eigenvectors are given by

$$\{W\}_m = \left\langle \dot{W}_{um} \; W_{um} \; \dot{W}_{\psi m} \; W_{\psi m} \right\rangle^T \tag{2.11}$$

in which $W_{um}, W_{\psi m}$ are the mode shapes corresponding to the transverse deflection u and bending angle ψ. Expanding (2.10) yields a system of four partial differential equations

$$\lambda_m \frac{A}{I} W_{um} = \frac{A}{I} \dot{W}_{um} \tag{2.12}$$

$$\lambda_m \frac{A}{I} \dot{W}_{um} = \left(-\frac{\kappa AG}{\rho I l^2} + \frac{q(1-\zeta)}{\rho I l} \right) W''_{um} + \frac{\kappa AG}{\rho I l} W'_{\psi m} \tag{2.13}$$

$$\lambda_m W_{\psi m} = \dot{W}_{\psi m} \tag{2.14}$$

$$\lambda_m \left(\dot{W}_{\psi m} - \frac{\Omega J_z}{\rho I} W_{\psi m} \right) = -\frac{\kappa AG}{\rho I l} W'_{um} - \frac{E}{\rho l^2} W''_{\psi m} + \frac{\kappa AG}{\rho I l} W_{\psi m} \tag{2.15}$$

Elimination of the time derivative yields the following coupled ordinary differential equations with undetermined coefficients.

$$(a_1 + a_2 \zeta) W''_{um} + a_3 W_{um} = a_4 W'_{\psi m} \tag{2.16}$$

$$a_5 W''_{\psi m} + a_6 W_{\psi m} = -a_4 W'_{um} \tag{2.17}$$

where

$$a_1 = \frac{\kappa AG}{\rho I l} - \frac{q}{\rho I l}, \qquad a_3 = \lambda_m^2 \frac{A}{I}, \qquad a_5 = \frac{E}{\rho l^2}$$

$$a_2 = \frac{q}{\rho I l}, \qquad a_4 = \frac{\kappa AG}{\rho I}, \qquad a_6 = \lambda_m^2 - \lambda_m \frac{\Omega J_z}{\rho I} - \frac{\kappa AG}{\rho I l}$$

The solution of the coupled ordinary differential equations is based on a series solution with no singularities in the range considered, $0<\zeta<1$.

$$W_{um} = \sum_{j=0}^{\infty} x_j \zeta^j \tag{2.18}$$

$$W_{\psi m} = \sum_{j=0}^{\infty} y_j \zeta^j \tag{2.19}$$

Substitution of (2.18) and (2.19) into (2.16) and (2.17) then evaluating yields four independent constants to be determined by boundary conditions, and recursion formulas to determine the remaining constants x_j and y_j. The recursion formulas are determined to be

$$x_{j+2} = \frac{-a_2(j+1)x_{j+1} - a_3 x_j + a_4(j+1)y_{j+1}}{a_1(j+1)(j+2)} \tag{2.20}$$

$$y_{j+2} = \frac{-a_6 y_j - a_4(j+1)x_{j+1}}{a_5(j+1)(j+2)} \tag{2.21}$$

Using the recursive relationships, (2.18) and (2.19) can be rewritten in the following form, collecting the unknown constants.

$$W_{um} = X_{x_0} x_0 + X_{y_0} y_0 + X_{x_1} x_1 + X_{y_1} y_1 \tag{2.22}$$

$$W_{\psi m} = Y_{x_0} x_0 + Y_{y_0} y_0 + Y_{x_1} x_1 + Y_{y_1} y_1 \tag{2.23}$$

where

$$X_{x_0} = 1 - \frac{a_3}{2a_1}\zeta^2 + \frac{a_2 a_3}{6a_1^2}\zeta^3 - \frac{2a_2^2 a_3 a_5 - a_1 a_3^2 a_5 - a_1 a_3 a_4^2}{24 a_1^3 a_5}\zeta^4 + \ldots$$

$$X_{y_0} = -\frac{a_4 a_6}{6a_1 a_5}\zeta^3 + \frac{a_2 a_4 a_6}{12 a_1^2 a_5}\zeta^4 + \ldots$$

$$X_{x_1} = \zeta - \frac{a_3 a_5 + a_4^2}{6a_1 a_5}\zeta^3 + \frac{a_2\left(a_3 a_5 + a_4^2\right)}{12 a_1^2 a_5}\zeta^4 + \ldots$$

$$X_{y_1} = \frac{a_4}{2a_1}\zeta^2 - \frac{a_2 a_4}{6a_1^2}\zeta^3 - \frac{-2a_2^2 a_4 a_5 + a_1 a_3 a_4 a_5 + a_1 a_4\left(a_1 a_6 + a_4^2\right)}{24 a_1^3 a_5}\zeta^4 + \ldots$$

$$Y_{x_0} = \frac{a_3 a_4}{6a_1 a_5}\zeta^3 - \frac{a_2 a_3 a_4}{24 a_1^2 a_5}\zeta^4 + \ldots$$

$$Y_{y_0} = 1 - \frac{a_6}{2a_5}\zeta^2 + \frac{a_2 a_6^2 + a_4^2 a_6}{24 a_1 a_5^2}\zeta^4 + \ldots$$

$$Y_{x_1} = -\frac{a_4}{2a_5}\zeta^2 + \frac{a_1 a_4 a_6 + a_3 a_4 a_5 + a_4^3}{24 a_1 a_5^2}\zeta^4 + \ldots$$

$$Y_{y_1} = \zeta - \frac{a_1 a_6 + a_4^2}{6a_1 a_5}\zeta^3 + \frac{a_2 a_4^2}{24 a_1^2 a_5}\zeta^4 + \ldots$$

X_{x_0}, X_{y_0}, X_{x_1}, X_{y_1} and Y_{x_0}, Y_{y_0}, Y_{x_1}, Y_{y_1} are infinite series requiring term by term evaluation because of the presence of the unknown natural frequency in the a_3 and a_6 terms. The natural frequencies are determined by applying boundary conditions to (2.22) and (2.23) and solving the resulting two equations for the natural frequencies. The natural frequencies are determined by setting the determinant to zero. The method is illustrated for the clamped-free beam case.

The boundary conditions for the clamped-free beam are the following:

$$W_{um}(0) = 0 \qquad W'_{\psi m}(1) = 0$$

$$W_{\psi m}(0) = 0 \qquad \frac{1}{l}W'_{um}(1) - W_{\psi m}(1) = 0$$

The result of imposing these boundary conditions upon (2.22) and (2.23) is that x_0 and y_0 vanish and x_1 and y_1 satisfy:

$$Y'_{x1}(1)x_1 + Y'_{y1}(1)y_1 = 0 \tag{2.24}$$

$$\left[\frac{1}{l}X'_{x1}(1)-Y_{x1}(1)\right]x_1+\left[\frac{1}{l}X'_{y1}(1)-Y_{y1}(1)\right]y_1=0 \tag{2.25}$$

Setting the determinant of (2.24) and (2.25) to zero yields the frequency equation for λ_m:

$$Y'_{x1}(1)\left[\frac{1}{l}X'_{y1}(1)-Y_{y1}(1)\right]-Y'_{y1}(1)\left[\frac{1}{l}X'_{x1}(1)-Y_{x1}(1)\right]=0 \tag{2.26}$$

The frequency equation is solved using MapleV for symbolic manipulation and a numerical root solver. The mode shapes for the free vibration of a clamped-free beam are determined by assuming x_1 to be unity and solving y_1 from one of (2.24) or (2.25). The mode shapes are determined from:

$$W_{um}=X_{x1}-\frac{Y'_{x1}(1)}{Y'_{y1}(1)}X_{y1} \tag{2.27}$$

$$W_{\psi m}=Y_{x1}-\frac{Y'_{x1}(1)}{Y'_{y1}(1)}Y_{y1} \tag{2.28}$$

The remainder of this chapter is devoted to presenting the results of the free vibration analysis of a spinning Timoshenko beam with distributed follower forces for the six classical boundary condition cases.

Numerical Analysis

The basic data employed in the following study is summarized as follows:

$$E=207\text{ GPa} \qquad \rho=7700\ \frac{\text{kg}}{\text{m}^3} \qquad l=1.0\text{ m}$$
$$G=77.6\text{ GPa} \qquad \kappa=0.9$$

The following non-dimensional parameters are used:

$\overline{\Omega}=\Omega/\omega_{10}$ - non-dimensional rotational speed

$\overline{q}=q/q_c$ - non-dimensional follower force

$\beta=\pi r_0/l$ - Rayleigh beam coefficient

where ω_{10} is the first at-rest natural frequency, q_c is the critical follower force beyond which the system loses its stability based on the Euler-Bernoulli beam theory, and r_0 is the radius of gyration of a circular cross section. The Rayleigh beam coefficient is a reflection of the stubbiness of the beam; as β increases the beam becomes more stubby.

To verify the frequency equations the natural frequencies of the spinning Timoshenko beams with zero follower forces are compared to the natural frequencies determined using the analytical formulas given by Zu and Han (1992). Their approach differs from the present method in two respects: their technique is valid for spinning Timoshenko beams with no follower forces and their solutions are based on transcendental functions. In order to make meaningful comparisons, the same system parameters as depicted previously are used in evaluating the solutions computed by the two methods. The presented data in the Tables 2.1, 2.2, 2.3, 2.4, 2.5, and 2.6 are for the case of $\overline{\Omega} = 2.5$, $\beta = 0.15$, and $q = 0\%$.

Clamped-Free Beam

The boundary conditions for a clamped-free beam are as follows:

$$W_{um}(0) = 0 \qquad W'_{\psi m}(1) = 0$$

$$W_{\psi m}(0) = 0 \qquad \frac{1}{l}W'_{um}(1) - W_{\psi m}(1) = 0$$

The frequency equation is:

$$Y'_{x1}(1)\left[X'_{y1}(1) - IY_{y1}(1)\right] - Y'_{y1}(1)\left[X'_{x1}(1) - IY_{y1}(1)\right] = 0$$

The mode shapes are given by:

$$W_{um} = X_{x1} - \frac{Y'_{x1}(1)}{Y'_{y1}(1)}X_{y1}$$

$$W_{\psi m} = Y_{x1} - \frac{Y'_{x1}(1)}{Y'_{y1}(1)}Y_{y1}$$

Table 2.1: Comparison of Analytical Natural Frequencies for Clamped-Free Beam with Zero Follower Forces, $\overline{\Omega} = 2.5$ and $\beta = 0.15$

Mode	Zu and Han (1992)	Current Work
1st	874.37151	874.37149
2nd	4930.89512	4930.89526
3rd	12081.73743	12081.73701
4th	20589.61384	20589.61454
5th	29832.75477	29832.75429

Table 2.1 gives the comparison of the natural frequency calculated using the above frequency equation to the natural frequencies calculated using the analytical formula of Zu and Han (1992). Figure 2.2 gives the variation of the natural frequency with the non-dimensional spin rate. Figure 2.3 gives the first three mode shapes for transverse deflection and bending deflection. Vibration mode shapes are independent of spin-rate and, hence, no spin-rate is given for Figure 2.3. Figure 2.4 gives the variation of natural frequency with distributed follower force for a clamped-free beam. Forward and backward precession frequencies are denoted by solid and dashed lines, respectively, in Figures 2.2, 2.3, and 2.4.

Table 2.1 shows excellent agreement between the analytical formula given by Zu and Han (1992) and the series solution used here. The small differences that occur between the values can be attributed to numerical errors. Recall that Zu and Han's formulas are based on transcendental equations requiring numerical root solvers to evaluate natural

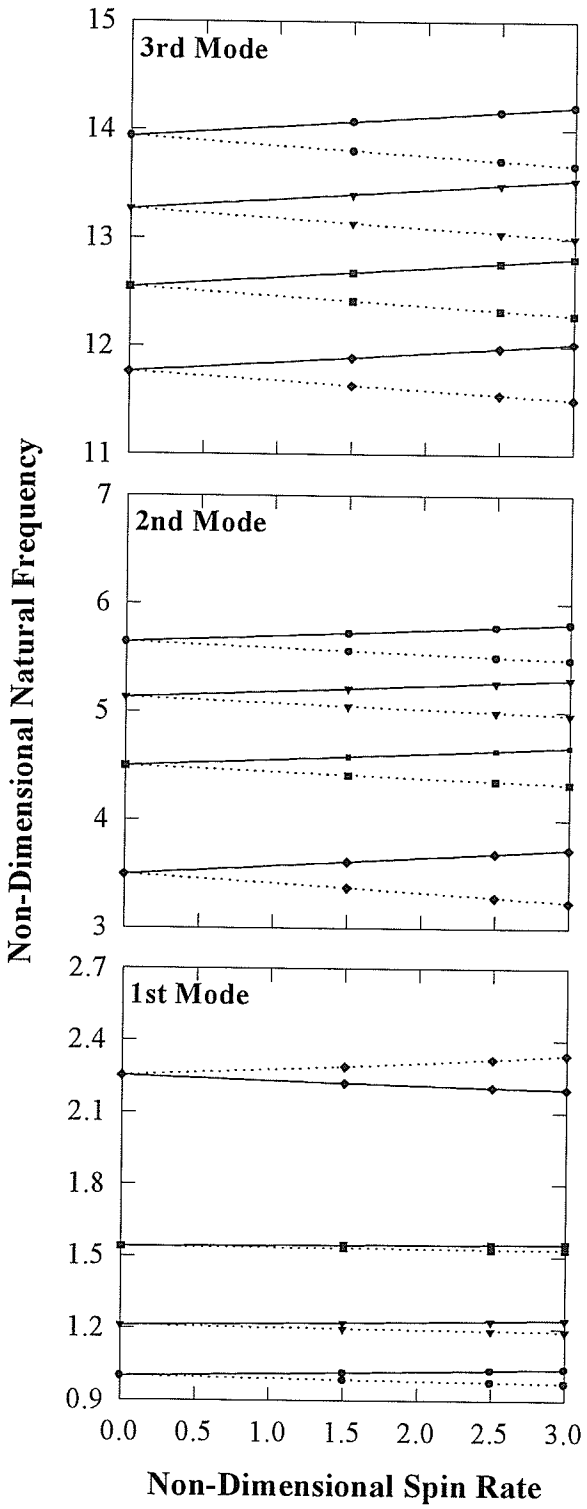

Figure 2.2: Variation of Natural Frequency with Spin Rate for Clamped-Free Beams
(• q=0%, ▾ q=25%, ▪ q=50%, ◆ q=75%)

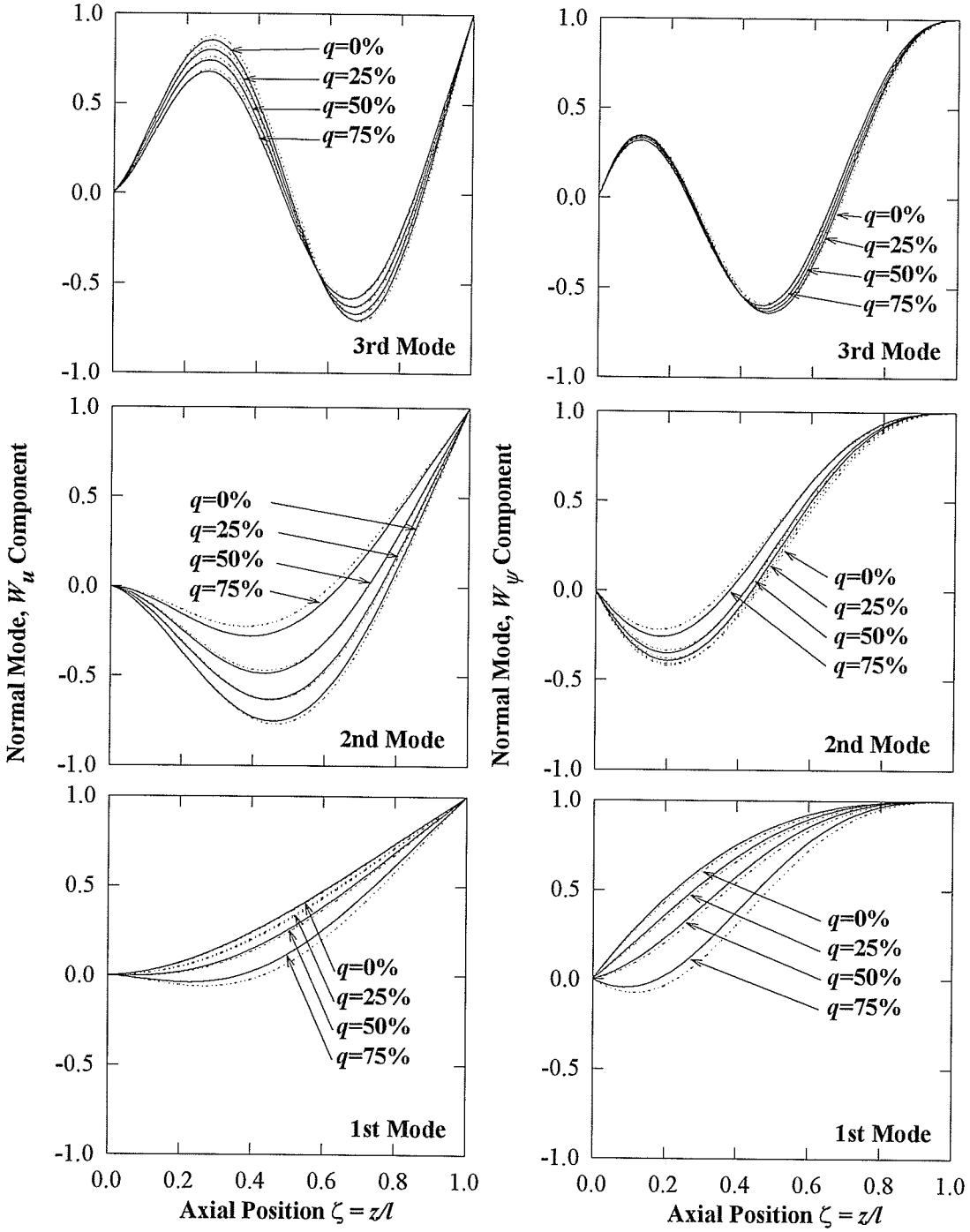

Figure 2.3: Free Vibration Mode Shapes for Clamped-Free Beams
(—— Forward Precession, ····· Backward Precession)

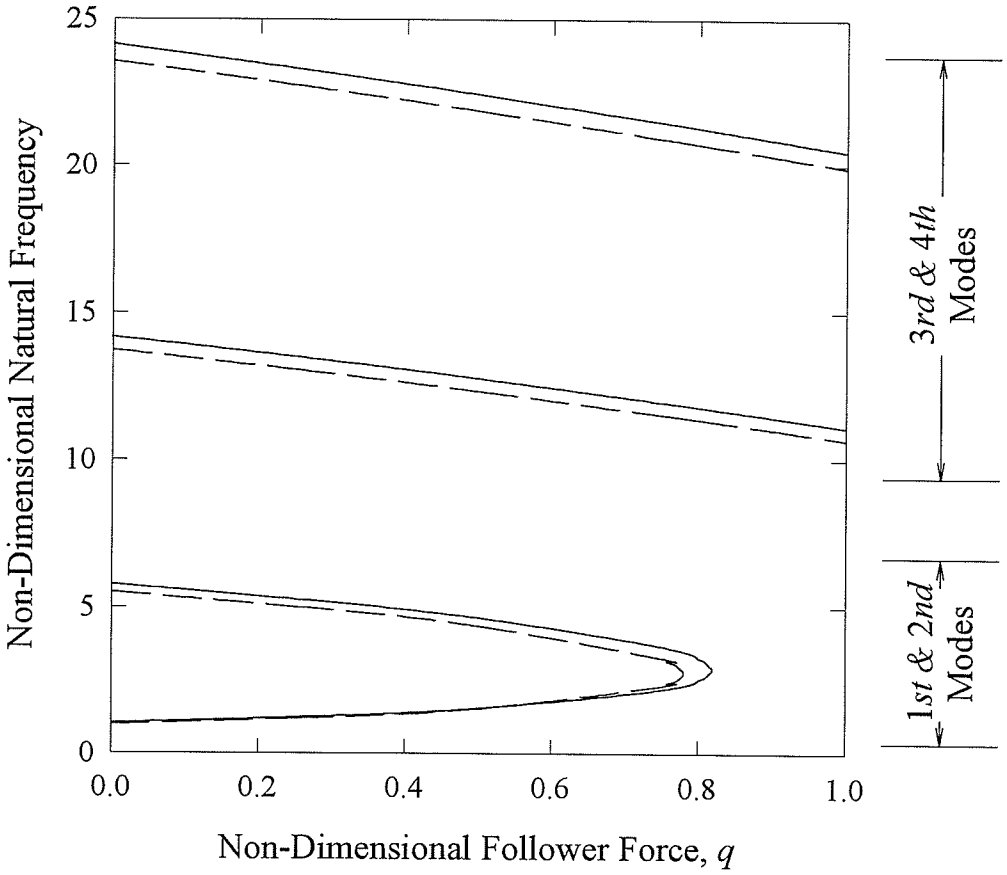

Figure 2.4: Variation of Natural Frequency with Distributed Follower Force for Clamped-Free Beams (—— Forward Precession, — – Backward Precession)

frequencies, and the series used here to compute the natural frequencies are truncated at 50 terms.

Figure 2.2 demonstrates a progressive stiffening of the beam as the follower force increases as shown by the increasing natural frequency. The plots of natural frequency also show the backward precession frequency being less than the forward precession for all modes except the fundamental. For the fundamental mode the precession frequencies experience a crossover at approximately 55% of critical follower load. At q=75% for the fundamental mode it can be seen that the backward precession frequencies are now greater than the forward precession frequencies.

Figure 2.3 clearly shows that the mode shapes for transverse and bending deflection conform to the clamped-free boundary conditions of the beam.

Figure 2.4 demonstrates a coalescence of the first and second natural frequencies at higher distributed follower forces. This coalescence of the first and second natural frequencies has been identified in literature sources as being indicative of the onset of a flutter-type instability. Of further interest is the fact that the onset of instability occurs at a magnitude of distributed follower force less than that predicted by the Euler-Bernoulli beam theory. As shown by Leipholz and Madan (1975), the critical follower force for a spinning, clamped-free Euler-Bernoulli beam is defined to be as follows:

$$q_c = 40.05 \cdot \frac{E \cdot I}{l^3}$$

Leipholz et al. identified this critical force as corresponding to the flutter-type instability. Figure 2.4 shows the critical follower force for forward precession to be 82% of the Euler-Bernoulli beam model prediction, and for backward precession, 78% of the Euler-Bernoulli beam model. Thus, the actual critical follower force determined by the Timoshenko beam model is less than the Euler-Bernoulli beam critical force. However, it should be noted that since the follower force was normalized using a critical follower force based on the Euler-Bernoulli beam theory, some distortion would be expected since the beam being investigated is considered stubby; it has a Rayleigh coefficient of 0.15.

Clamped-Clamped Beam

The boundary conditions for a clamped-clamped beam are as follows:

$$W_{um}(0) = 0 \qquad W_{um}(1) = 0$$
$$W_{\psi m}(0) = 0 \qquad W_{\psi m}(1) = 0$$

The frequency equation is:

$$X_{x1}(1)Y_{y1}(1) - X_{y1}(1)Y_{x1}(1) = 0$$

The mode shapes are given by:

$$W_{um} = X_{x1} - \frac{X_{x1}(1)}{X_{y1}(1)} X_{y1}$$

$$W_{\psi m} = Y_{x1} - \frac{X_{x1}(1)}{X_{y1}(1)} Y_{y1}$$

Table 2.2 gives the comparison of the natural frequency calculated using the above frequency equation to the natural frequencies calculated using the analytical formula of Zu and Han (1992). Figure 2.5 gives the variation of the natural frequency with the non-dimensional spin rate. Figure 2.6 gives the first three mode shapes for transverse deflection and bending deflection. Vibration mode shapes are independent of spin-rate and, hence, no spin-rate is given for Figure 2.6. Figure 2.7 gives the variation of natural frequency with distributed follower force for a clamped-clamped beam. Forward and backward precession frequencies are denoted by solid and dashed lines, respectively, in Figures 2.5, 2.6, and 2.7.

Table 2.2: Comparison of Analytical Natural Frequencies for Clamped-Clamped Beam with Zero Follower Forces, $\overline{\Omega} = 2.5$ and $\beta = 0.15$

Mode	Zu and Han (1992)	Current Work
1st	4955.25431	4955.25428
2nd	11883.07423	11883.07445
3rd	20186.05360	20186.05281
4th	29188.36882	29188.37016
5th	38600.90490	38600.90372

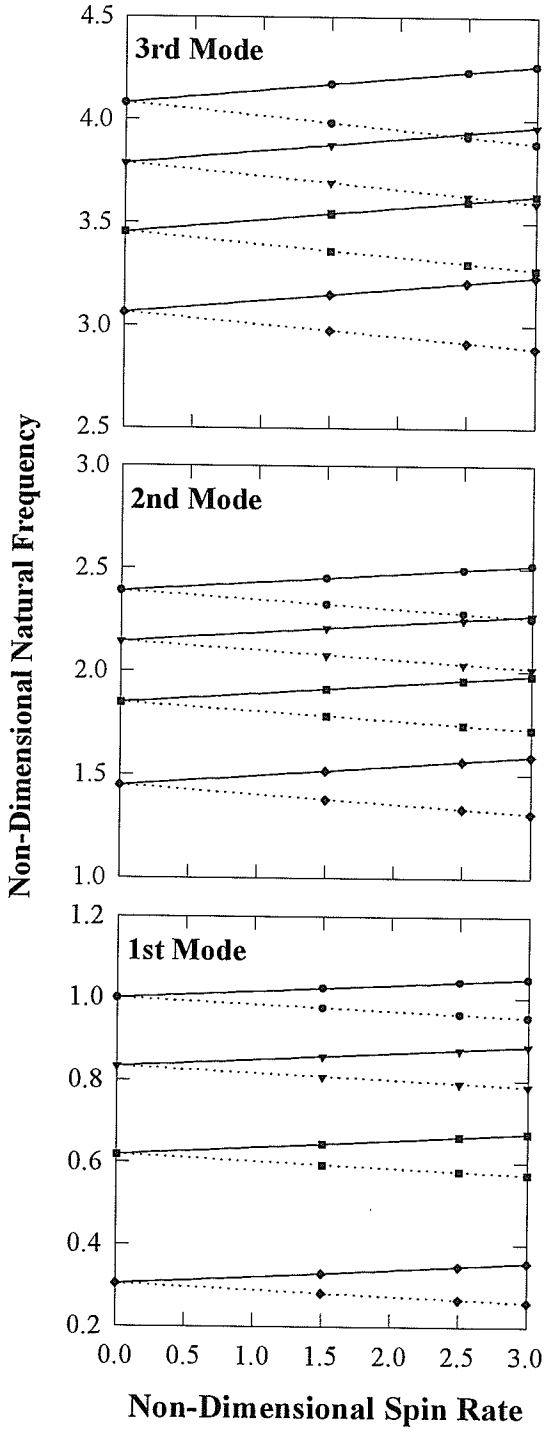

Figure 2.5: Variation of Natural Frequency with Spin Rate for Clamped-Clamped Beams
(• q=0%, ▾ q=25%, ▪ q=50%, ◆ q=75%)

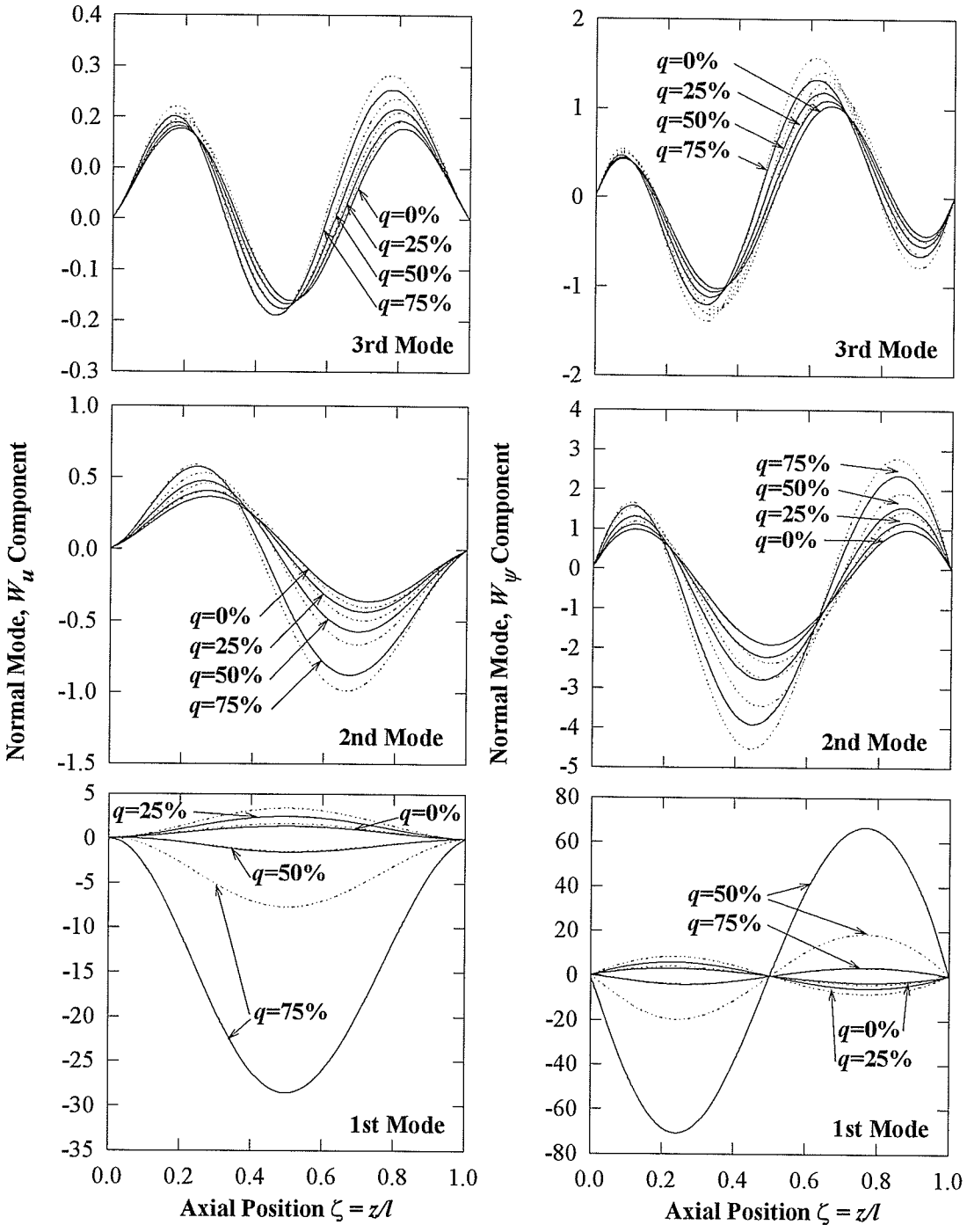

Figure 2.6: Free Vibration Mode Shapes for Clamped-Clamped Beams
(—— Forward Precession, ····· Backward Precession)

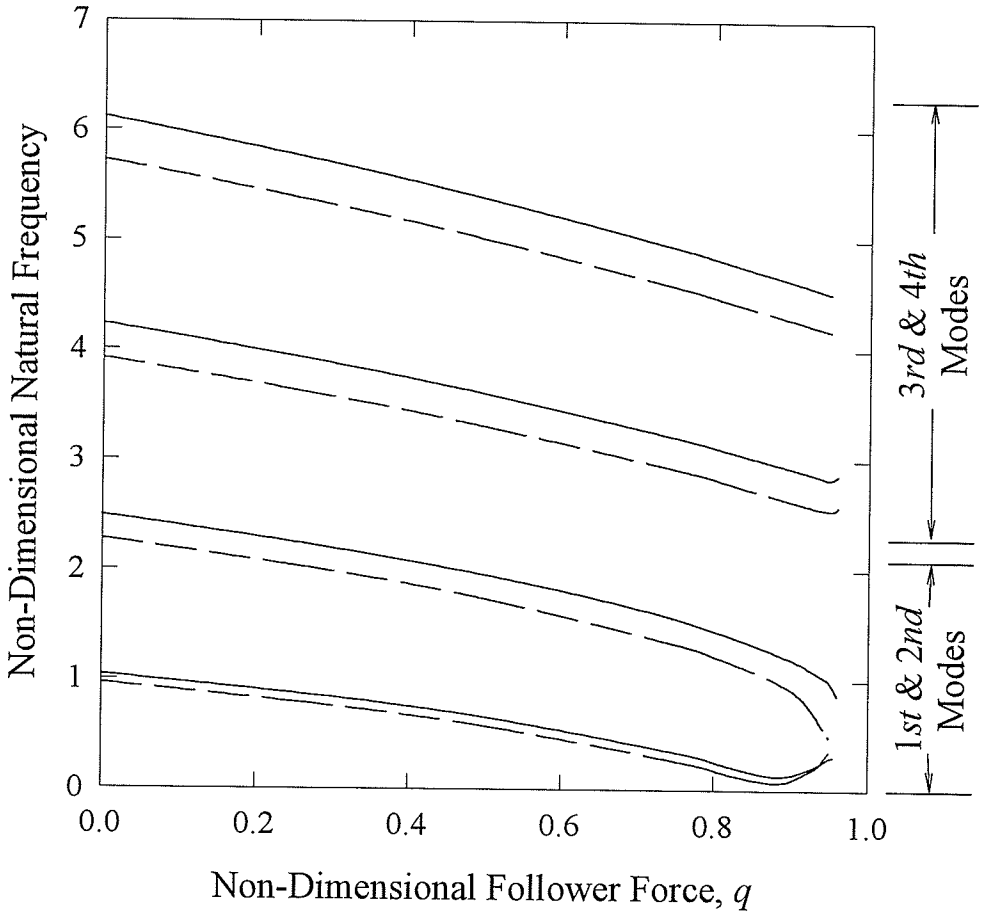

Figure 2.7: Variation of Natural Frequency with Distributed Follower Force for Clamped-Clamped Beams (—— Forward Precession, — – Backward Precession)

Table 2.2 shows excellent agreement between the analytical frequency equation given by Zu and Han (1992) and the series solution of the current work. As with the clamped-free case differences can be attributed to numerical solution differences.

Figure 2.5 shows a trend reversal from that found for the clamped-free beam. For increasing follower force it is found that the natural frequencies decrease indicating a structural softening of a clamped-clamped beam. Unlike the clamped-free beam, the forward precession frequencies are greater than the backward precession frequencies for every vibration mode.

Figure 2.6 clearly shows that the mode shapes for transverse and bending deflection conform to the clamped-clamped boundary conditions of the beam.

Figure 2.7 does not demonstrate a coalescence of the natural frequencies even though the 1st and 2nd modes appear to meet, nor do these frequencies approach zero at higher q. However, based on our numerical experimentation, it is found that beyond 95.5% of the critical force, the solution of the frequency equation abruptly diverges, indicating the onset of an instability. This is true for both the forward and backward precession frequencies. Leipholz and Madan (1975) showed using the Euler-Bernoulli beam theory, that the instability is of the divergence-type, and they calculated the critical follower force for a spinning clamped-clamped beam to be:

$$q_c = 80.255 \cdot \frac{E \cdot I}{l^3}$$

Figure 2.7 shows the critical follower force for forward precession to be 95.5% of the Euler-Bernoulli beam model prediction, and for backward precession, 95.5% of the Euler-Bernoulli beam model. Once again, the actual critical follower force determined by the Timoshenko beam model is less than the Euler-Bernoulli beam critical force.

Clamped-Hinged Beam

The boundary conditions for a clamped-hinged beam are as follows:

$$W_{um}(0) = 0 \qquad W_{um}(1) = 0$$
$$W_{\psi m}(0) = 0 \qquad W'_{\psi m}(1) = 0$$

The frequency equation is:

$$X_{x1}(1)Y'_{y1}(1) - X_{y1}(1)Y'_{x1}(1) = 0$$

The mode shapes are given by:

$$W_{um} = X_{x1} - \frac{X_{x1}(1)}{X_{y1}(1)} X_{y1}$$

$$W_{\psi m} = Y_{x1} - \frac{X_{x1}(1)}{X_{y1}(1)} Y_{y1}$$

Table 2.3: Comparison of Analytical Natural Frequencies for Clamped-Hinged Beam with Zero Follower Forces, $\overline{\Omega} = 2.5$ and $\beta = 0.15$

Mode	Zu and Han (1992)	Current Work
1st	3649.37840	3649.37840
2nd	10380.84750	10380.84750
3rd	18770.65521	18770.65521
4th	27985.23674	27985.23674
5th	37623.24857	37623.24857

Table 2.3 gives the comparison of the natural frequency calculated using the above frequency equation to the natural frequencies calculated using the analytical formula of Zu and Han (1992). Figure 2.8 shows the variation of the natural frequency with the non-dimensional spin rate. Figure 2.9 depicts the first three mode shapes for transverse deflection and bending deflection. Vibration mode shapes are independent of spin-rate and, hence, no spin-rate is given for Figure 2.9. Figure 2.10 gives the variation of natural frequency with distributed follower force for a clamped-hinged beam. Forward and backward precession frequencies are denoted by solid and dashed lines, respectively, for Figure 2.8, 2.9, and 2.10.

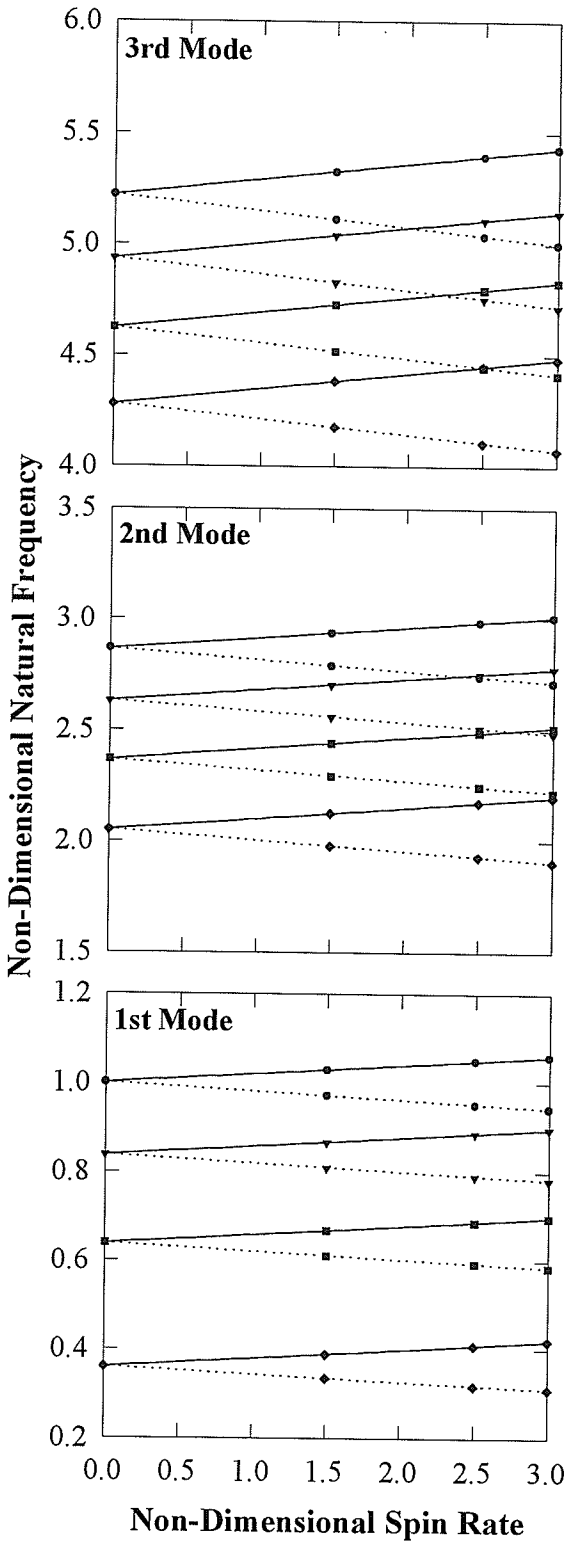

Figure 2.8: Variation of Natural Frequency with Spin Rate for Clamped-Hinged Beams
(• q=0%, ▾ q=25%, ▪ q=50%, ◆ q=75%)

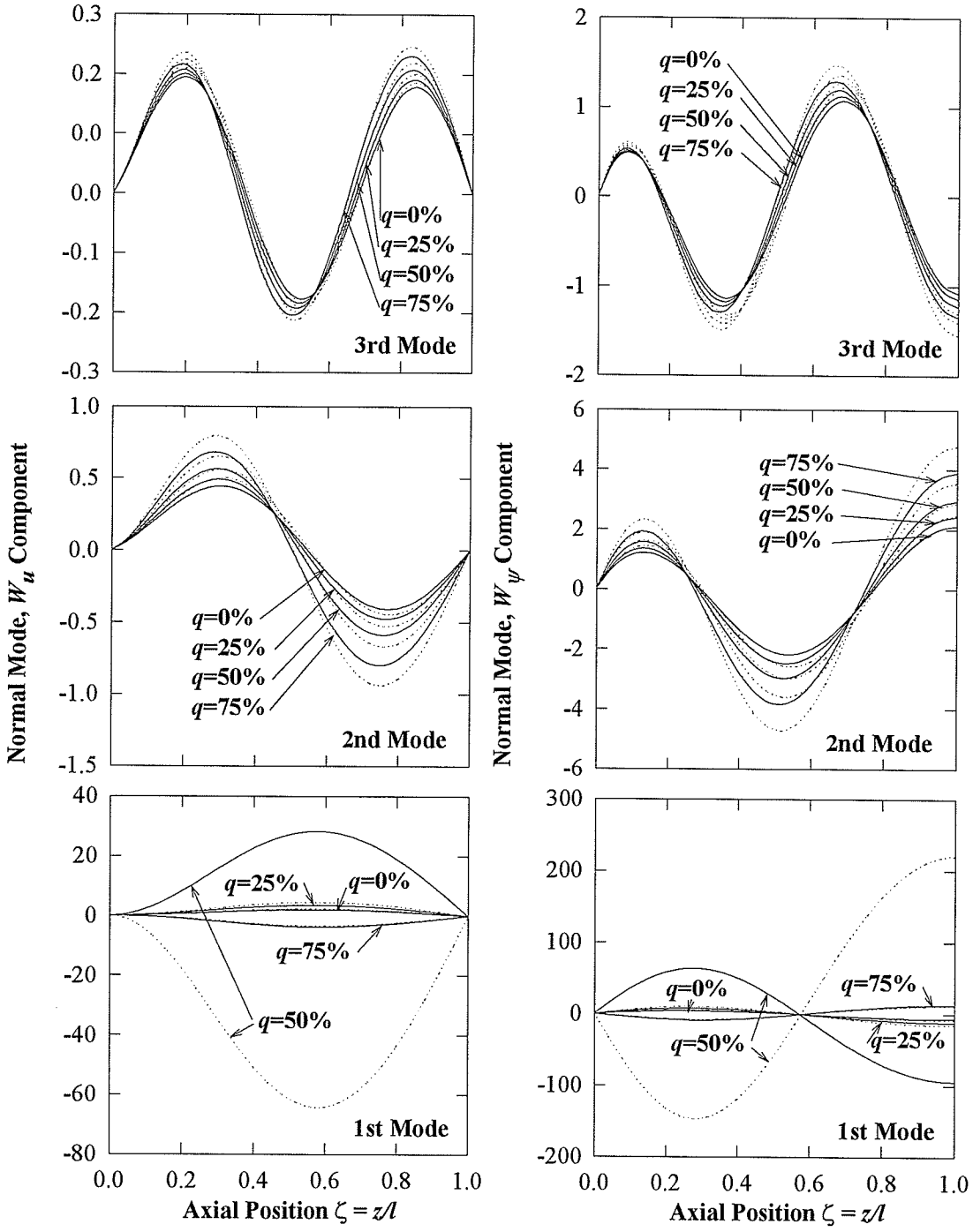

Figure 2.9: Free Vibration Modes Shapes for Clamped-Hinged Beams
(—— Forward Precession, ····· Backward Precession)

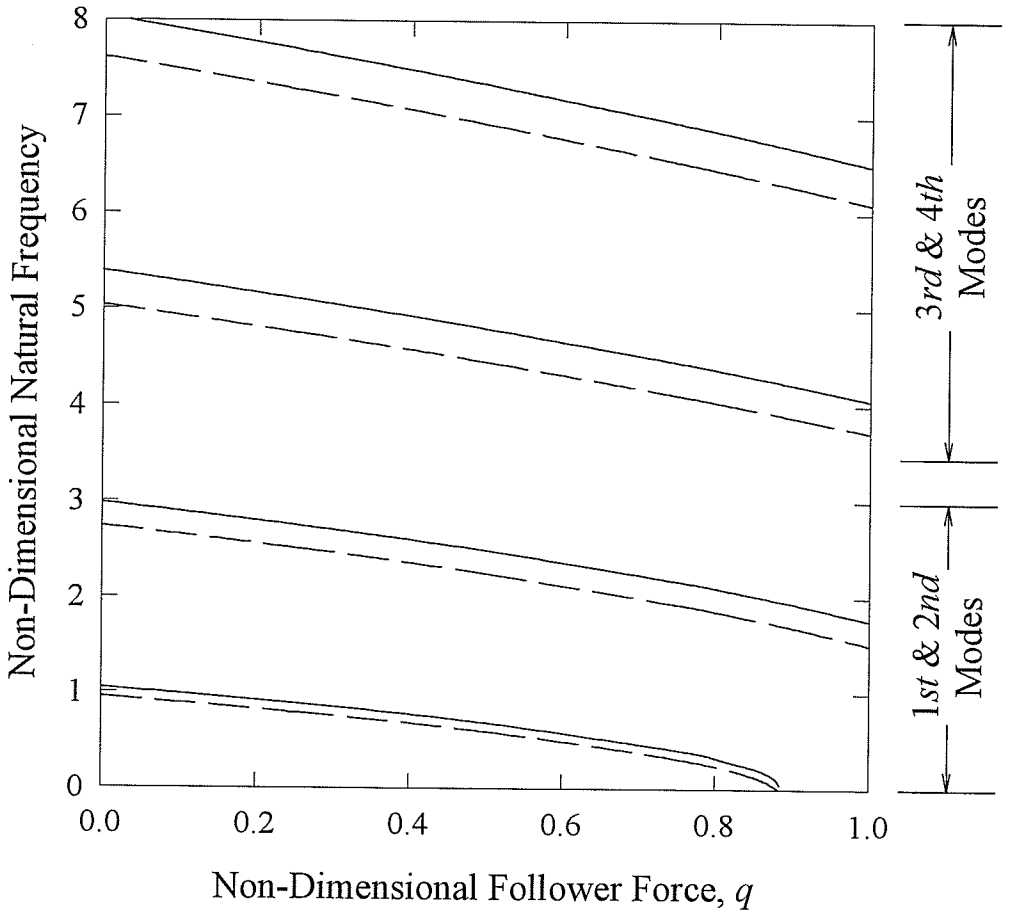

Figure 2.10: Variation of the Natural Frequency with Distributed Follower Force for Clamped-Hinged Beams (—— Forward Precession, — – Backward Precession)

Table 2.3 shows excellent agreement between the two analytical formulas. As usual, the small differences can be attributed to the approximations used to determine the natural frequencies.

Figure 2.8 shows the natural frequency for a spinning clamped-hinged beam decreases as the distributed follower force increases. This is the same trend identified with the clamped-clamped beam. As with the clamped-clamped beam the backward precession frequency is less than the forward precession frequency for all vibration modes.

Figure 2.9 clearly shows that the mode shapes for transverse and bending deflection conform to the clamped-hinged boundary conditions of the beam.

Figure 2.10 shows the fundamental frequency of the clamped-hinged beam falling off to zero as the critical follower force is approached. This has been identified as the divergence-type of instability. Based on the Euler-Bernoulli beam theory, the critical follower force for a spinning clamped-hinged beam (Leipholz and Madan, 1975) is defined to be as follows:

$$q_c = 57.007 \cdot \frac{E \cdot I}{l^3}$$

Leipholz et al. identified this critical force as corresponding to a divergence-type instability. Figure 2.10 shows the critical follower force for forward precession to be 88.5% of the Euler-Bernoulli beam model prediction, and for backward precession, 88.2% of the Euler-Bernoulli beam model. As before, the actual critical follower force computed by the Timoshenko beam model is less than the Euler-Bernoulli beam critical force.

Hinged-Hinged Beam

The boundary conditions for a hinged-hinged beam are as follows:

$$W_{um}(0) = 0 \qquad W_{um}(1) = 0$$
$$W'_{\psi m}(0) = 0 \qquad W'_{\psi m}(1) = 0$$

The frequency equation is:

$$X_{y0}(1)Y'_{x1}(1) - X_{x1}(1)Y'_{y0}(1) = 0$$

The mode shapes are given by:

$$W_{um} = X_{y0} - \frac{X_{y0}(1)}{X_{x1}(1)} X_{x1}$$

$$W_{ym} = Y_{y0} - \frac{X_{y0}(1)}{X_{y1}(1)} Y_{x1}$$

Table 2.4 gives the comparison of the natural frequency calculated using the above frequency equation to the natural frequencies calculated using the analytical formula of Zu and Han (1992). Figure 2.11 gives the variation of the natural frequency with the non-dimensional spin rate. Figure 2.12 gives the first three mode shapes for transverse deflection and bending deflection. Vibration mode shapes are independent of spin-rate and, hence, no spin-rate is given for Figure 2.12. Figure 2.13 gives the variation of natural frequency with distributed follower force for a hinged-hinged beam. Forward and backward precession frequencies are denoted by solid and dashed lines, respectively, in Figures 2.11, 2.12, and 2.13.

Table 2.4: Comparison of Analytical Natural Frequencies for Hinged-Hinged Beam with Zero Follower Forces, $\overline{\Omega} = 2.5$ and $\beta = 0.15$

Mode	Zu and Han (1992)	Current Work
1st	2460.73225	2460.73225
2nd	8789.83407	8789.83407
3rd	17242.27617	17242.27617
4th	26698.70175	26698.70175
5th	36607.52426	36607.52426

Table 2.4 shows excellent agreement between the two analytical formulas. As usual, the small differences are attributed to the numerical evaluation of the natural frequencies.

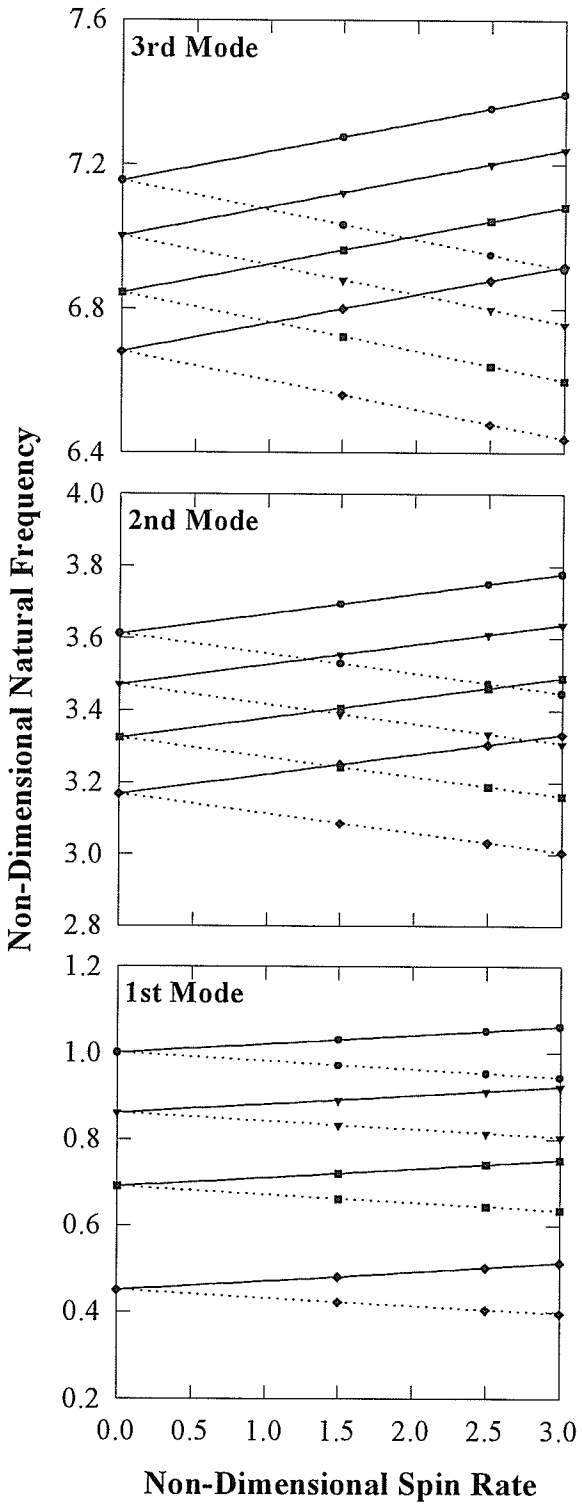

Figure 2.11: Variation of Natural Frequency with Spin Rate for Hinged-Hinged Beams
(• q=0%, ▾ q=25%, ▪ q=50%, ◆ q=75%)

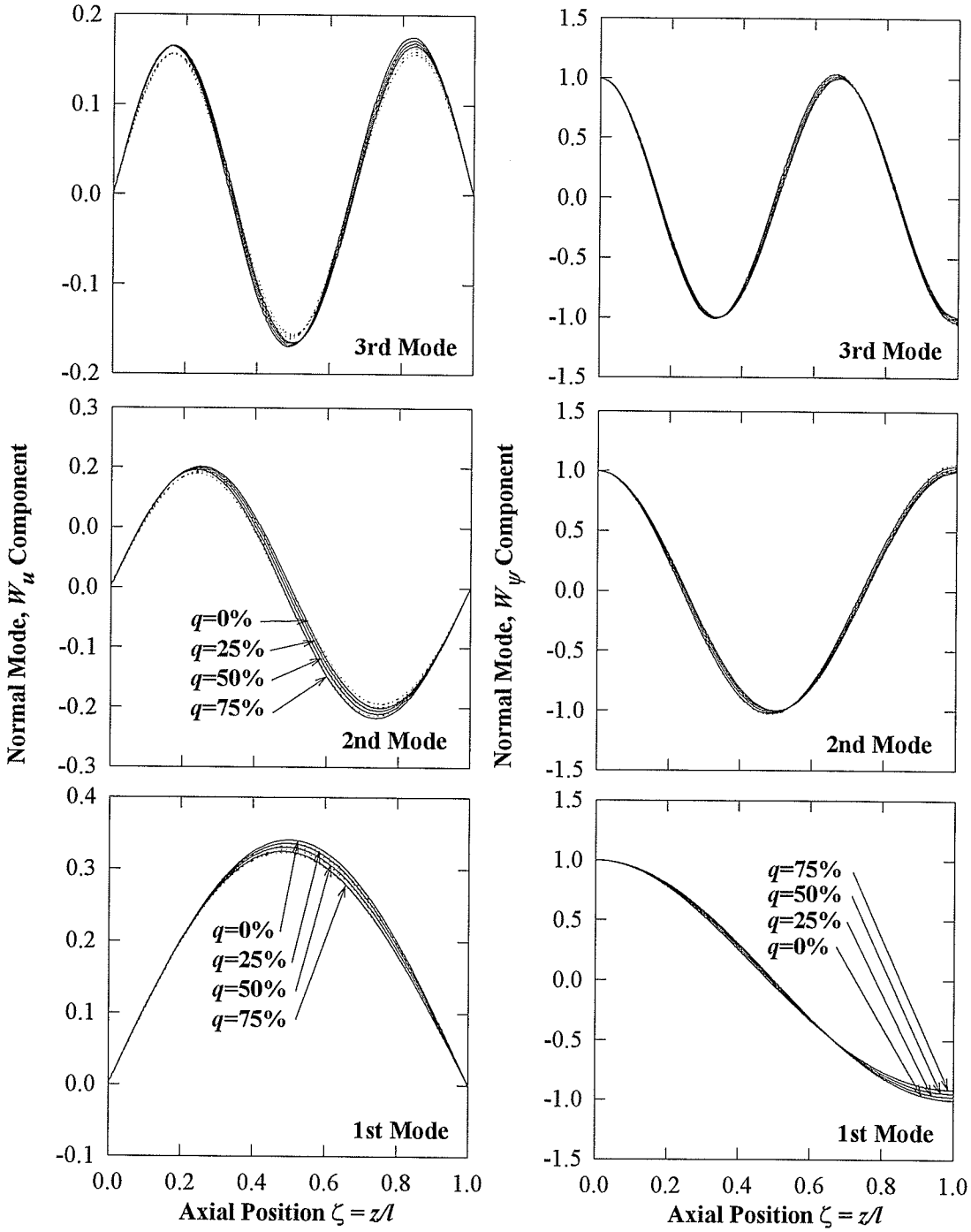

Figure 2.12: Free Vibration Modes Shapes for Hinged-Hinged Beams
(—— Forward Precession, ····· Backward Precession)

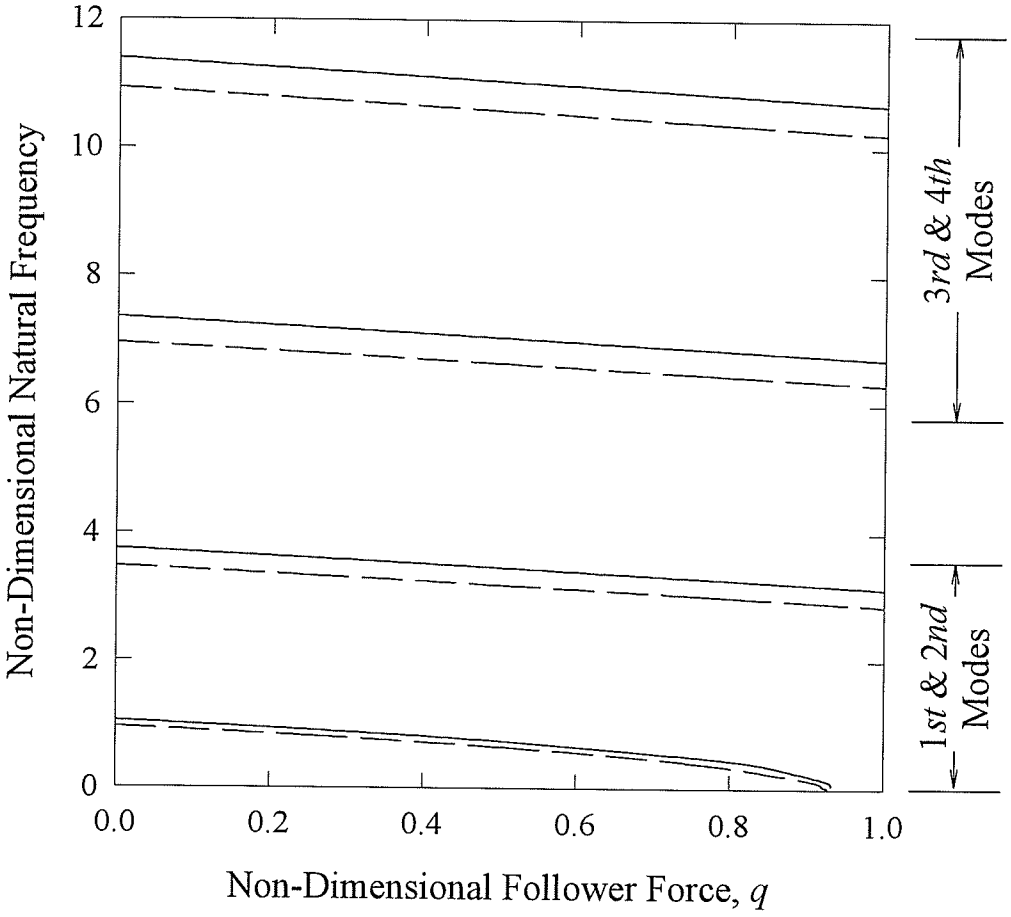

Figure 2.13: Variation of Natural Frequency with Distributed Follower Force for Hinged-Hinged Beams (—— Forward Precession, — – Backward Precession)

Figure 2.11 demonstrates the same trend in natural frequency with follower force as seen with the clamped-clamped and clamped-hinged boundary condition cases. The natural frequency decrease with increasing distributed follower force.

Figure 2.12 clearly shows that the mode shapes for transverse and bending deflection conform to the hinged-hinged boundary conditions of the beam.

Figure 2.13 shows the divergence-type of instability at a critical follower force less than the Euler-Bernoulli critical force. Based on the Euler-Bernoulli beam theory, the

critical follower force for a spinning hinged-hinged beam (Leipholz and Madan, 1975) is defined to be as follows:

$$q_c = 18.9564 \cdot \frac{E \cdot I}{l^3}$$

Leipholz et al. identified this critical force as corresponding to a divergence-type instability. Figure 2.13 shows the critical follower force for forward precession to be 93.2% of the Euler-Bernoulli beam model prediction, and for backward precession, 92.7% of the Euler-Bernoulli beam model. Once again, the actual critical follower force determined by the Timoshenko beam model is less than the Euler-Bernoulli beam critical force.

Hinged-Free Beam

The boundary conditions for a hinged-free beam are as follows:

$$W_{um}(0) = 0 \qquad W'_{\psi m}(1) = 0$$

$$W'_{\psi m}(0) = 0 \qquad \frac{1}{l} W'_{um}(1) - W_{\psi m}(1) = 0$$

The frequency equation is:

$$Y'_{y0}(1)\left[X'_{x1}(1) - lY_{x1}(1)\right] - Y'_{x1}(1)\left[X'_{y0}(1) - lY_{y0}(1)\right] = 0$$

The mode shapes are given by:

$$W_{um} = X_{y0} - \frac{Y'_{y0}(1)}{Y'_{x1}(1)} X_{x1}$$

$$W_{\psi m} = Y_{y0} - \frac{Y'_{y0}(1)}{Y'_{x1}(1)} Y_{x1}$$

Table 2.5 gives the comparison of the natural frequency calculated using the above frequency equation to the natural frequencies calculated using the analytical formula of Zu and Han (1992). Figure 2.14 gives the variation of the natural frequency with the non-dimensional spin rate. Figure 2.15 gives the first three mode shapes for transverse deflection and bending deflection. Vibration mode shapes are independent of spin-rate and, hence, no spin-rate is given for Figure 2.15. Figure 2.16 give the variation of natural frequency with distributed follower force for a hinged-free beam. Forward and backward precession frequencies are denoted by solid and dashed lines, respectively, in Figures 2.14, 2.15, and 2.16.

Table 2.5: Comparison of Analytical Natural Frequencies for Hinged-Free Beam with Zero Follower Forces, $\overline{\Omega} = 2.5$ and $\beta = 0.15$

Mode	Zu and Han (1992)	Current Work
1st	121.43163	121.43163
2nd	4067.51499	4067.51499
3rd	11265.55076	11265.55076
4th	20138.05309	20138.05309
5th	29755.43417	29755.43416
6th	39668.95669	39668.95669

Table 2.5 shows excellent agreement between the two analytical formulas. As before, the small differences can be attributed to the approximations used to determine the natural frequencies.

As with the previous three boundary condition cases, Figure 2.14 shows the natural frequency decreasing with increasing distributed follower force for the hinged-free beam.

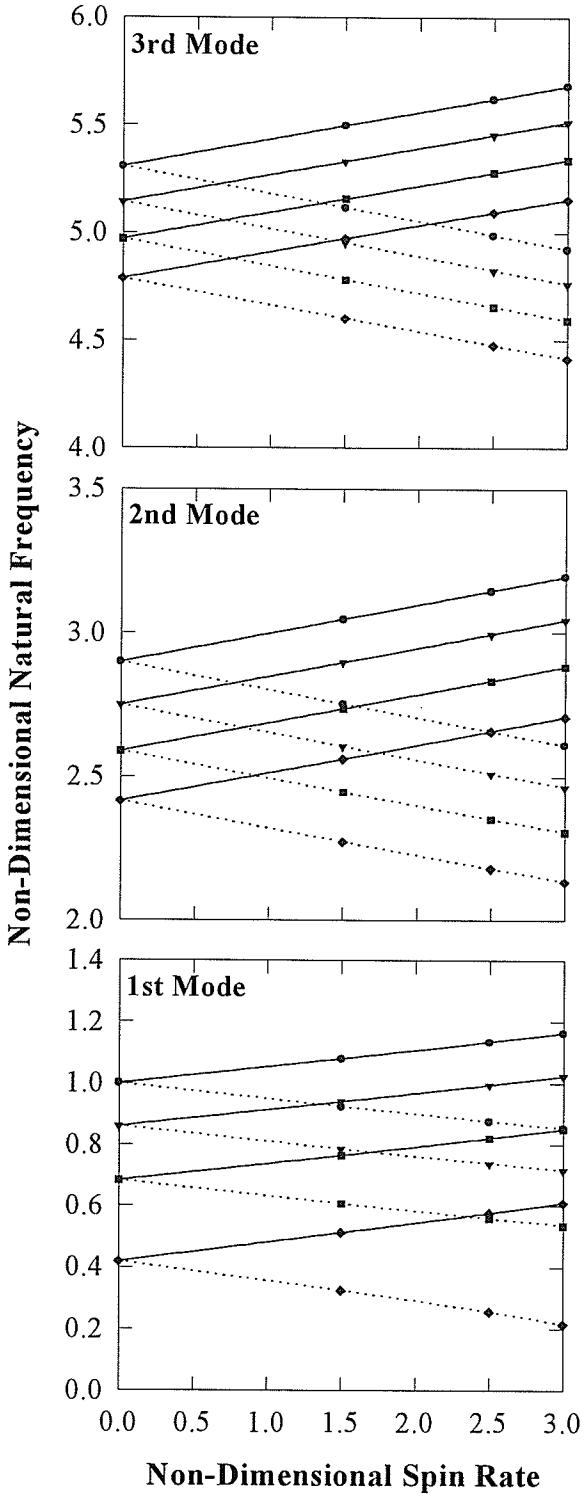

Figure 2.14: Variation of Natural Frequency with Spin Rate for Hinged-Free Beams
(• q=0%, ▾ q=25%, ▪ q=50%, ◆ q=75%)

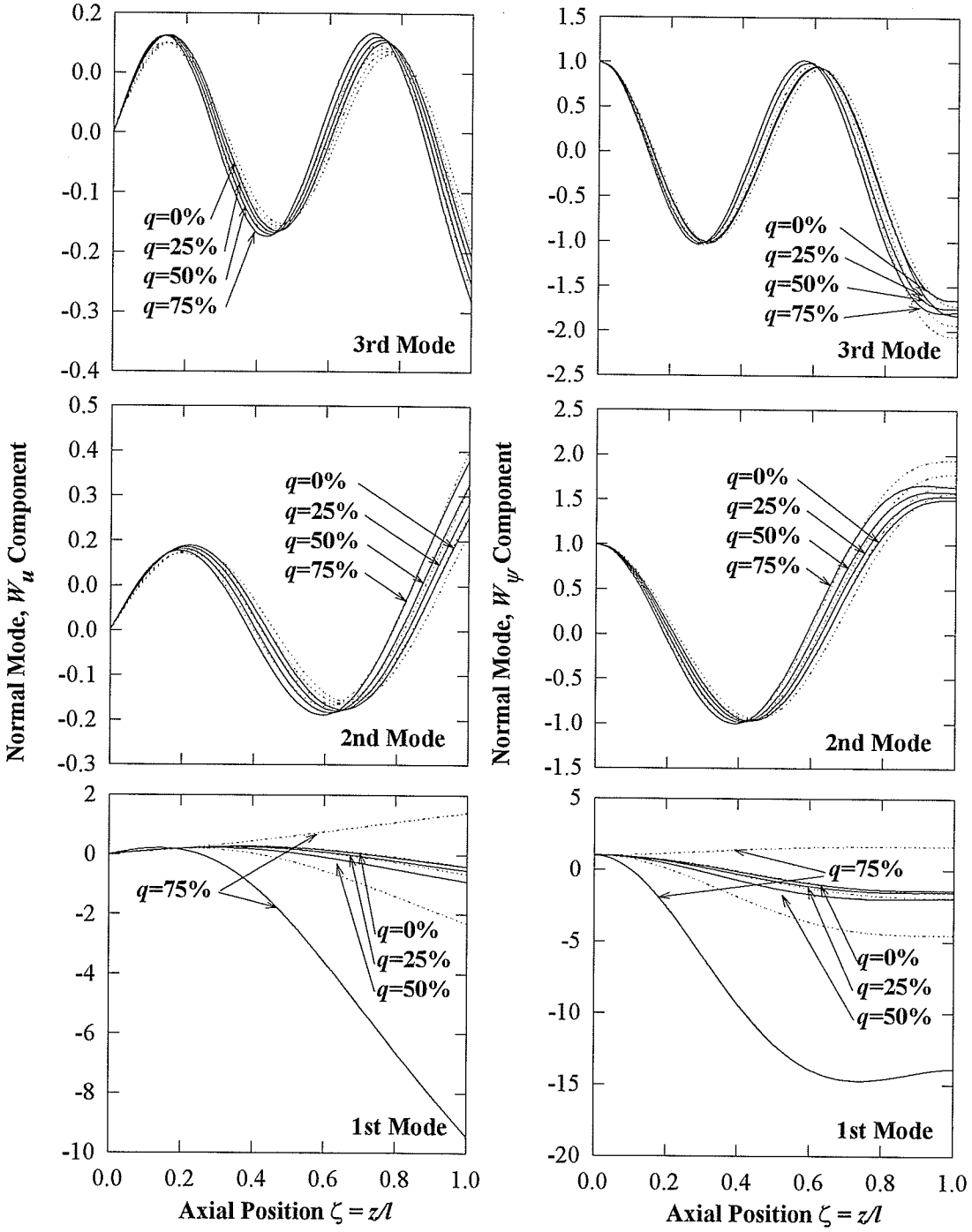

Figure 2.15: Free Vibration Modes Shapes for Hinged-Free Beams
(—— Forward Precession, ····· Backward Precession)

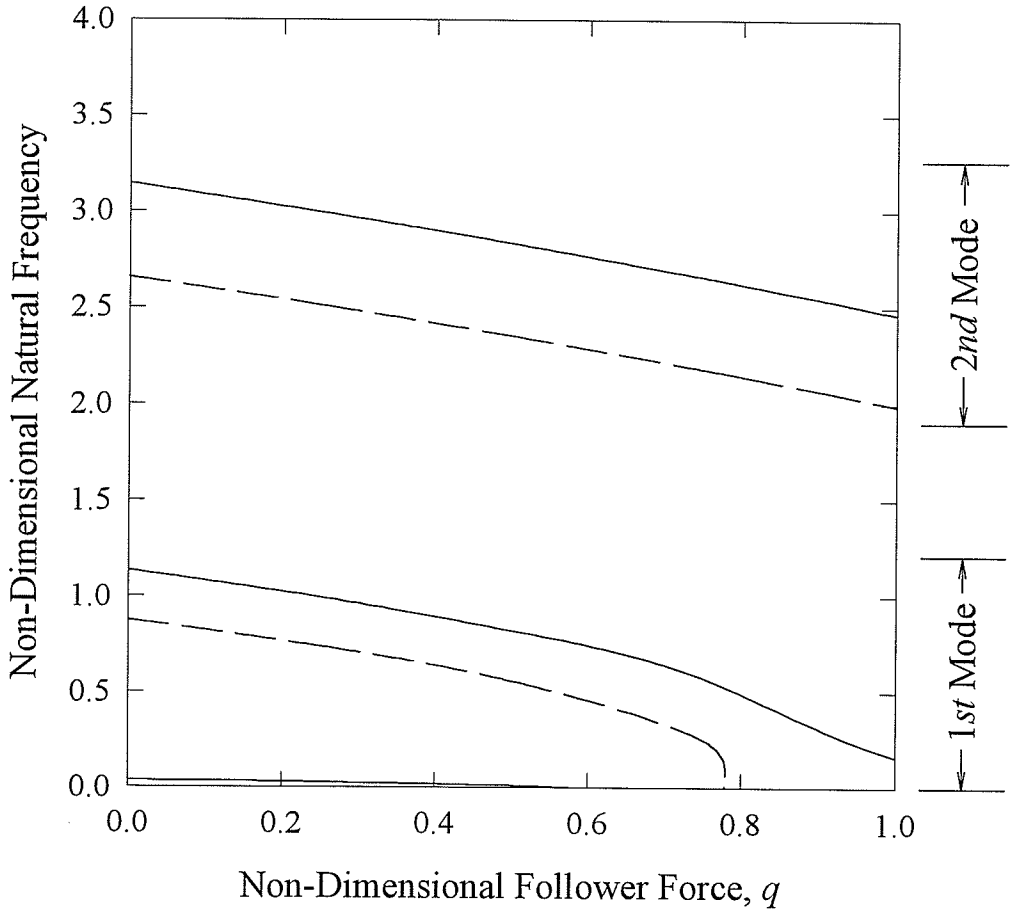

Figure 2.16: Variation of Natural Frequency with Distributed Follower Force for Hinged-Free Beams (—— Forward Precession, — – Backward Precession)

Figure 2.15 clearly shows that the mode shapes for transverse and bending deflection conform to the hinged-free boundary conditions of the beam.

Figure 2.16 demonstrates divergence-type instability in both the forward and backward precession modes. Based on the Euler-Bernoulli beam theory, the critical follower force for a spinning hinged-free beam (Leipholz and Madan, 1975) is defined to be as follows:

$$q_c = 30.571 \cdot \frac{E \cdot I}{l^3}$$

Leipholz et al. identified this critical force as corresponding to a divergence-type instability. Figure 2.16 shows the critical follower force for forward precession to be 57.5% of the Euler-Bernoulli beam model prediction, and for backward precession, 77.8% of Euler-Bernoulli beam model. As before, the actual critical follower force determined by the Timoshenko beam model is less than the Euler-Bernoulli beam critical force.

Free-Free Beam

The boundary conditions for a free-free beam are as follows:

$$W'_{\psi m}(0) = 0 \qquad W'_{\psi m}(1) = 0$$

$$\frac{1}{l}W'_{um}(0) - W_{\psi m}(0) = 0 \qquad \frac{1}{l}W'_{um}(1) - W_{\psi m}(1) = 0$$

The frequency equation is:

$$Y'_{xo}(1)\left(X'_{y0}(1) + lX'_{x1}(1) - lY_{y0} - l^2 Y_{x1}(1)\right) - \left(X'_{x0}(1) - lY_{x0}(1)\right)\left(Y'_{y0}(1) + lY'_{x1}(1)\right) = 0$$

The mode shapes are given by:

$$W_{um} = X_{x0} - \frac{Y'_{x0}(1)}{Y'_{y0}(1) + lY'_{x1}(1)}\left(X_{y0} + lX_{x1}\right)$$

$$W_{um} = Y_{x0} - \frac{Y'_{x0}(1)}{Y'_{y0}(1) + lY'_{x1}(1)}\left(Y_{y0} + lY_{x1}\right)$$

Table 2.6 gives the comparison of the natural frequency calculated using the above frequency equation to the natural frequencies calculated using the analytical formula of Zu and Han (1992). Figure 2.17 gives the variation of the natural frequency with the non-dimensional spin rate. Figure 2.18 gives the first three mode shapes for transverse deflection and bending deflection. Vibration mode shapes are independent of spin-rate and, hence, no spin-rate is given for Figure 2.18 Forward and backward precession

frequencies are denoted by solid and dashed lines, respectively, in Figures 2.17, 2.18 and 2.19.

Table 2.6: Comparison of Analytical Natural Frequencies for Free-Free Beam with Zero Follower Forces, $\overline{\Omega} = 2.5$ and $\beta = 0.15$

Mode	Zu and Han (1992)	Current Work
1st	671.92224	671.92224
2nd	6283.94220	6283.94220
3rd	14231.46039	14231.46039
4th	23460.35395	23460.35395
5th	33197.19736	33197.19739
6th	43099.43934	43099.43937

Table 2.6 shows excellent agreement between the two analytical formulas. As before, the small differences can be attributed to the approximations used to determine the natural frequencies.

Figure 2.17 shows the same trend as most of the boundary condition cases of decreasing natural frequency with increasing follower force. The backward precession frequency is less than the forward precession frequency for all modes. The backward precession of the fundamental mode shows indications of an asymptotic relationship existing with spin-rate. At q=75% the backward precession frequency is almost unchanged with increasing spin-rate.

Figure 2.18 clearly shows that the mode shapes for transverse and bending deflection conform to the free-free boundary conditions of the beam.

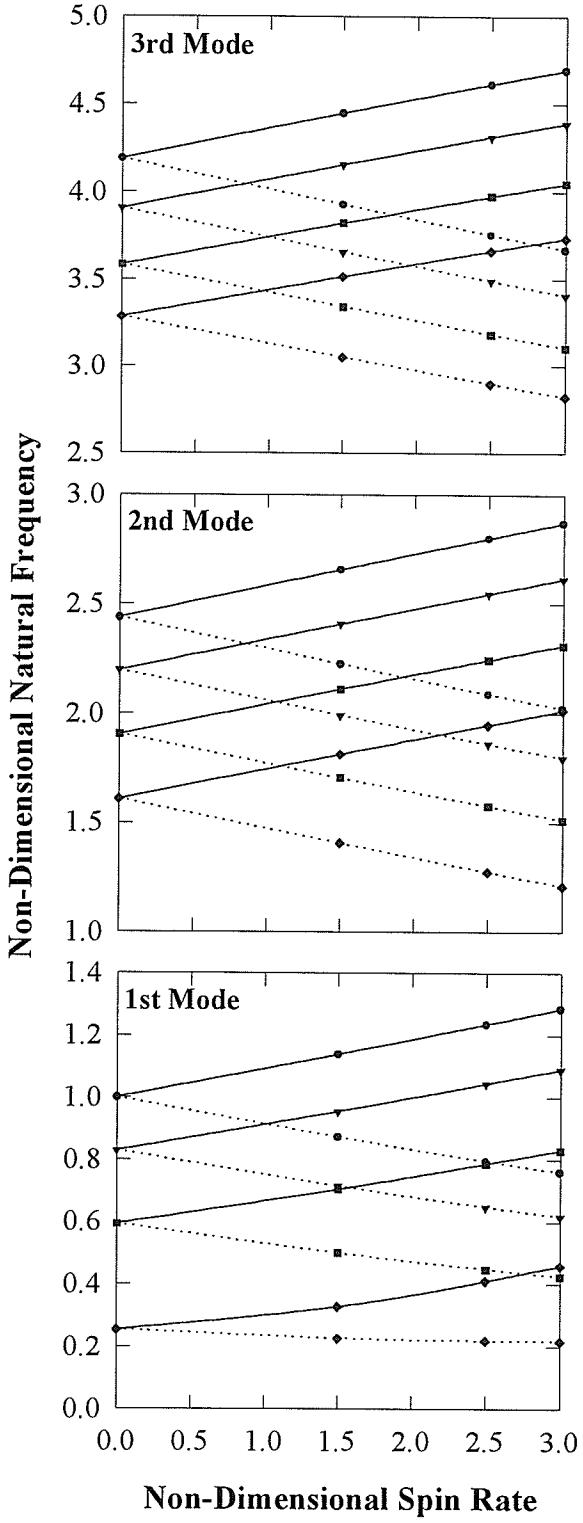

Figure 2.17: Variation of Natural Frequency with Spin Rate for Free-Free Beams
(• q=0%, ▾ q=25%, ▪ q=50%, ◆ q=75%)

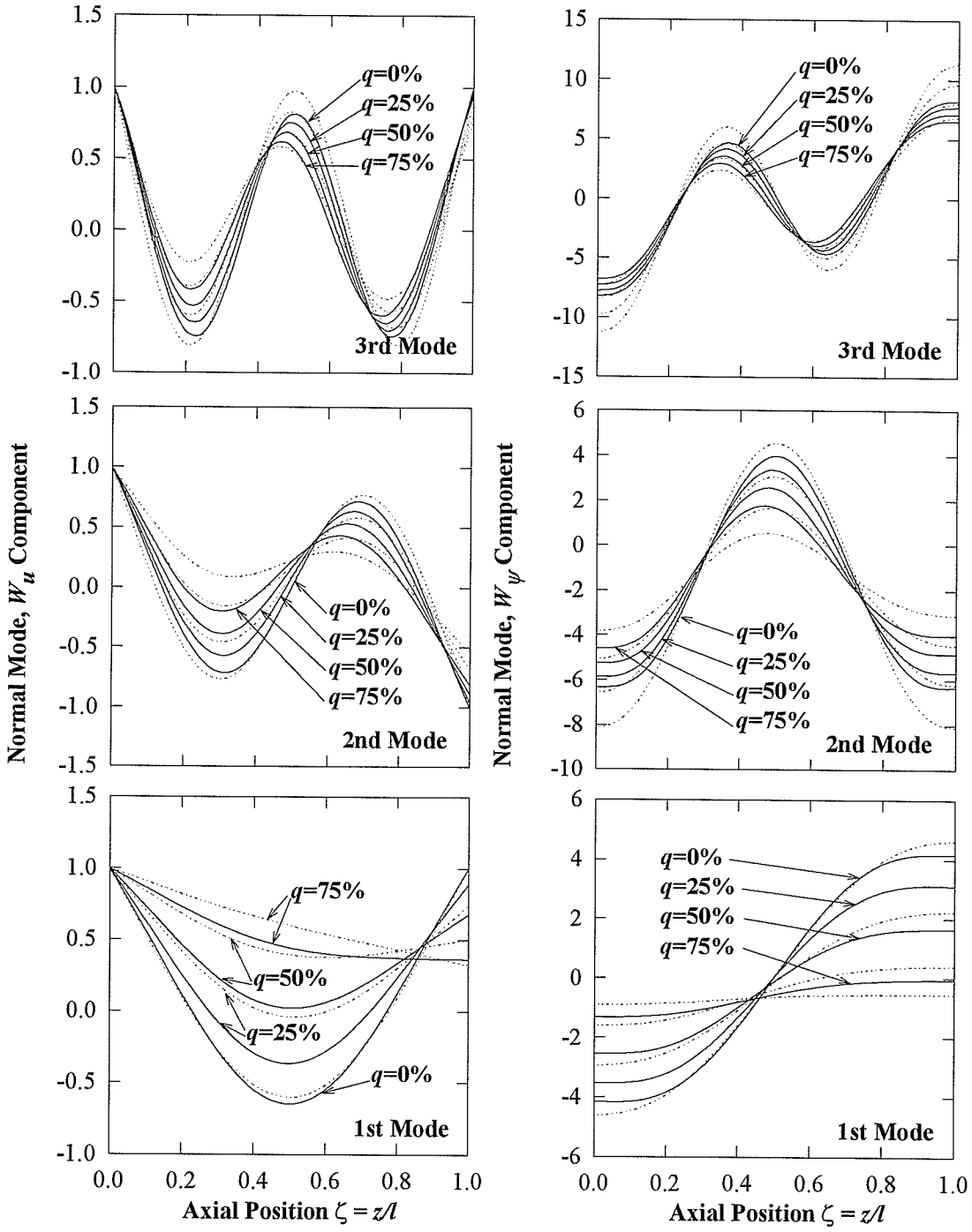

Figure 2.18: Free Vibration Modes Shapes for Free-Free Beams
(—— Forward Precession, ····· Backward Precession)

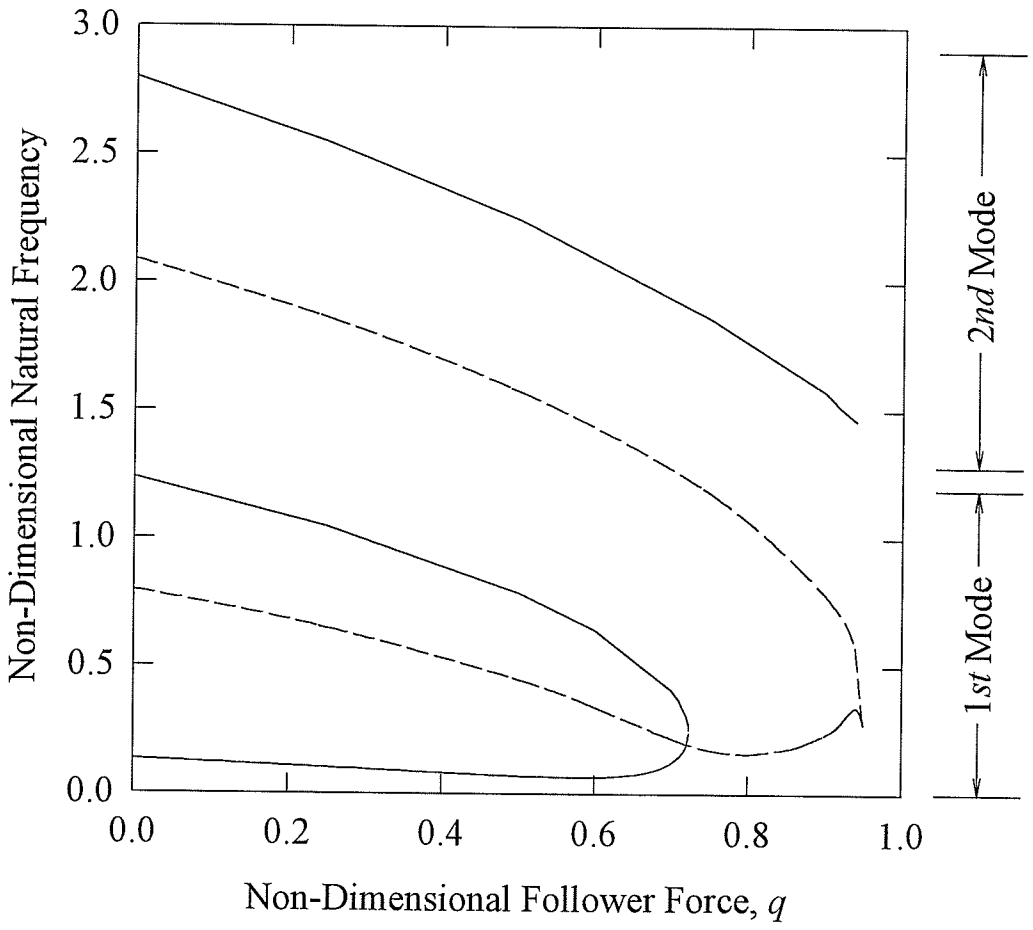

Figure 2.19: Variation of Natural Frequency with Distributed Follower Force for Free-Free Beams (—— Forward Precession, — – Backward Precession)

Figure 2.19 demonstrate coalescence of the lowest modes for both the forward and backward precession frequencies. Based on the Euler-Bernoulli beam theory, the critical follower force for a spinning free-free beam (Leipholz and Madan, 1975) is defined to be as follows:

$$q_c = 80.25 \cdot \frac{E \cdot I}{l^3}$$

The forward precession shows flutter-type instability occurring at 72.4% of Euler-Bernoulli critical follower force. The backward precession shows flutter-type instability occurring at 94% of Euler-Bernoulli critical follower force. A large number of terms

(>100) were required in the series solution in order to achieve coalescence of the precessions frequencies. Once again, the actual critical follower force determined by the Timoshenko beam model is less than the Euler-Bernoulli beam critical force.

Chapter 3

Forced Vibration Analysis

Introduction

Chapter 3 covers the forced vibration of a spinning Timoshenko beam under the influence of a distributed follower force and an applied transverse distributed load. Physical symmetries in the sense of Betti-Maxwell reciprocity theorem are eliminated by the presence of distributed follower forces in the beam system. The removal of the physical symmetries results in the beam problem being non-selfadjoint. Forced vibration analysis is achieved by the use of adjoint analysis and modal expansion.

Adjoint Analysis

The non-selfadjoint nature of the problem under investigation requires the analysis of the adjoint system to be carried out before the forced vibration analysis can be performed. The free vibration analysis required the analysis of the real system for eigenvalues and eigenvectors. The adjoint system will also be analyzed for the eigenvalues and eigenvectors. The real and adjoint eigenpairs are then related by the biorthonormality conditions as follows:

$$\left\langle [M]\{W\}_m, \{W^*\}_n \right\rangle = \delta_{mn}, \qquad m,n = \pm 1, \pm 2, \ldots \tag{3.1}$$

$$\left\langle [K]\{W\}_m, \{W^*\}_n \right\rangle = \lambda_m \delta_{mn}, \qquad m,n = \pm 1, \pm 2, \ldots \tag{3.2}$$

where δ_{mn} is the Kronecker delta function, and $\langle a, b \rangle$ denotes the inner product of a and b. The adjoints of the mass and stiffness matrix operators are (Han and Zu, 1995):

$$\left[M^*\right]=\left[M\right]=\begin{bmatrix} 0 & A/I & 0 & 0 \\ A/I & 0 & 0 & 0 \\ 0 & 0 & 0 & 1 \\ 0 & 0 & 1 & -\Omega\dfrac{J_z}{\rho I} \end{bmatrix} \tag{3.3}$$

$$\left[K^*\right]=\begin{bmatrix} A/I & 0 & 0 & 0 \\ 0 & \left(-\dfrac{\kappa AG}{\rho I l^2}+\dfrac{q(1-\zeta)}{\rho I l}\right)\dfrac{\partial^2}{\partial\zeta^2}-\dfrac{2q}{\rho I l}\dfrac{\partial}{\partial\zeta} & 0 & \dfrac{\kappa AG}{\rho I l}\dfrac{\partial}{\partial\zeta} \\ 0 & 0 & 1 & 0 \\ 0 & -\dfrac{\kappa AG}{\rho I l}\dfrac{\partial}{\partial\zeta} & 0 & -\dfrac{E}{\rho l^2}\dfrac{\partial^2}{\partial\zeta^2}+\dfrac{\kappa AG}{\rho I} \end{bmatrix} \tag{3.4}$$

Defining the state vector of the adjoint system to be:

$$\left\{W^*\right\}_n=\left\langle \dot{W}^*_{un}\ W^*_{un}\ \dot{W}^*_{\psi m}\ W^*_{\psi m}\right\rangle^T \tag{3.5}$$

in which $\left\{W^*\right\}_n$ denotes the nth eigenvector of the adjoint system and W^*_{um}, $W^*_{\Psi n}$ are the nth eigenvector components pertaining to transverse deflections are bending angle, respectively. The boundary conditions of the adjoint system are determined by the following adjoint analysis. The following inner product calculation yields the boundary conditions of the adjoint system.

$$\begin{aligned} \left\langle [\mathrm{K}]\{W\}_m,\left\{W^*\right\}_n\right\rangle = {} & \frac{A}{I}\int_0^1 \dot{W}^*_{un}\dot{W}_{um}d\zeta+\left(\frac{Q}{\rho I l^2}-\frac{\kappa AG}{\rho I l^2}\right)\int_0^1 W^*_{un}W''_{um}d\zeta \\ & +\frac{q}{\rho I l}\int_0^1 W^*_{un}\left\{\left[(1-\zeta)W'_{um}\right]'+\zeta W'_{um}\right\}d\zeta+\frac{\kappa AG}{\rho I l}\int_0^1 W^*_{un}W'_{\psi m}d\zeta \\ & +\int_0^1 \dot{W}^*_{\psi n}\dot{W}_{\psi m}d\zeta-\frac{\kappa AG}{\rho I l}\int_0^1 W^*_{\psi m}W'_{um}d\zeta-\frac{E}{\rho l^2}\int_0^1 W^*_{\psi n}W''_{\psi m}d\zeta \\ & +\frac{\kappa AG}{\rho I}\int_0^1 W^*_{\psi n}W_{\psi m}d\zeta \end{aligned} \tag{3.6}$$

and

$$\begin{aligned}\left\langle \{W\}_m, \left[K^*\right]\left\{W^*\right\}_n \right\rangle = {} & \frac{A}{I}\int_0^1 \dot{W}_{un}^* \dot{W}_{um} d\zeta + \left(\frac{Q}{\rho I l^2} - \frac{\kappa AG}{\rho I l^2}\right)\int_0^1 W_{un}''^* W_{um} d\zeta \\ & + \frac{q}{\rho I l}\left\{\int_0^1 \left[(1-\zeta) - \zeta W_{un}'^*\right]' W_{um}' d\zeta - \int_0^1 W_{un}'^* W_{um} d\zeta\right\} \\ & + \frac{\kappa AG}{\rho I l}\int_0^1 W_{\psi m}'^* W_{um} d\zeta + \int_0^1 \dot{W}_{\psi m}^* \dot{W}_{\psi m} d\zeta - \frac{\kappa AG}{\rho I l}\int_0^1 W_{un}'^* W_{\psi m} d\zeta \\ & - \frac{E}{\rho l^2}\int_0^1 W_{\psi n}''^* W_{\psi m} d\zeta + \frac{\kappa AG}{\rho I}\int_0^1 W_{\psi n}^* W_{\psi m} d\zeta\end{aligned} \tag{3.7}$$

Integrating by parts yields:

$$\left\langle [K]\{W\}_m, \left\{W^*\right\}_n \right\rangle = \left\langle \{W\}_m, \left[K^*\right]\left\{W^*\right\}_n \right\rangle + B.C.$$

in which the boundary condition terms are:

$$\begin{aligned} B.C. = {} & \left(\frac{Q}{\rho I l^2} - \frac{\kappa AG}{\rho I l^2}\right)\left(W_{un}'^* W_{um}\Big|_0^1 - W_{un}^* W_{um}'\Big|_0^1\right) \\ & + \frac{q}{\rho I l}\left[(1-\zeta)\left(W_{un}'^* W_{um}\Big|_0^1 - W_{un}^* W_{um}'\Big|_0^1\right) - W_{un}^* W_{um}\Big|_0^1\right] \\ & + \frac{\kappa AG}{\rho I l}\left(W_{\psi n}^* W_{um}\Big|_0^1 - W_{un}^* W_{\psi m}\Big|_0^1\right) - \frac{E}{\rho l^2}\left(W_{\psi n}'^* W_{\psi m}\Big|_0^1 - W_{\psi n}^* W_{\psi m}'\Big|_0^1\right)\end{aligned} \tag{3.8}$$

Applying the boundary conditions of the real system to equation (3.8) and setting equal to zero yields the boundary conditions of the adjoint system.

Having determined the adjoint system boundary conditions, the eigenpairs of the adjoint system are obtained by the method used for the free vibration analysis of Chapter 2. The eigenproblem associated with the adjoint system is given by

$$\lambda_n^* \left[M^*\right]\left\{W^*\right\}_n = \left[K^*\right]\left\{W^*\right\}_n, \qquad n = \pm 1, \pm 2, \ldots \tag{3.9}$$

where λ_n^* are the nth eigenvalue of the adjoint system, $\left[M^*\right]$ and $\left[K^*\right]$ are the adjoint differential operators defined previously, and $\left\{W^*\right\}_n$ represents the nth eigenvector of the adjoint system. Expanding (3.9) gives

$$\lambda_n^* \frac{A}{I} W_{un}^* = \frac{A}{I} \dot{W}_{un}^* \tag{3.10}$$

$$\lambda_n^* \frac{A}{I} \dot{W}_{un}^* = \left[-\frac{\kappa AG}{\rho I l^2} + \frac{q(1-\zeta)}{\rho I l} \right] W_{un}''^* - \frac{2q}{\rho I l} W_{un}'^* + \frac{\kappa AG}{\rho I l} W_{\psi m}'^* \tag{3.11}$$

$$\lambda_n^* W_{\psi m}^* = \dot{W}_{\psi m}^* \tag{3.12}$$

$$\lambda_n^* \left(\dot{W}_{\psi m}^* - \frac{\Omega J_z}{\rho I} W_{\psi m}^* \right) = -\frac{\kappa AG}{\rho I l} W_{un}'^* - \frac{E}{\rho l^2} W_{\psi m}''^* + \frac{\kappa AG}{\rho I l} W_{\psi m}^* \tag{3.13}$$

Eliminating the time derivatives as before, equations (3.10) - (3.13) can be expressed as two coupled ordinary differential equations with undetermined coefficients:

$$\left(a_1^* + a_2^* \zeta\right) W_{un}''^* + a_7^* W_{un}'^* + a_3^* W_{un}^* = a_4^* W_{\psi m}'^* \tag{3.14}$$

$$a_5^* W_{\psi m}''^* + a_6^* W_{\psi m}^* = -a_4^* W_{un}'^* \tag{3.15}$$

where

$$a_1^* = \frac{\kappa AG}{\rho I l}, \qquad a_3^* = \lambda_n^{*2} \frac{A}{I}, \qquad a_5^* = \frac{E}{\rho l^2}$$

$$a_2^* = \frac{q}{\rho I l}, \qquad a_4^* = \frac{\kappa AG}{\rho I}, \qquad a_6^* = \lambda_n^{*2} - \lambda_n^* \frac{\Omega J_z}{\rho I} - \frac{\kappa AG}{\rho I}, \qquad a_7^* = \frac{2q}{\rho I l}$$

The ordinary differential equations are solved in the same fashion as for free vibration. A series expansion solution is assumed:

$$W_{un}^* = \sum_{j=0}^{\infty} x_j^* \zeta^j \tag{3.16}$$

$$W_{\psi m}^* = \sum_{j=0}^{\infty} y_j^* \zeta^j \tag{3.17}$$

The recursive relationships resulting from substituting (3.16) and (3.17) into (3.14) and (3.15) are:

$$x_{j+2}^* = -\frac{1}{a_1^*(j+1)(j+2)} \left\{ \left[a_2^* j(j+1) + a_7^*(j+1) \right] x_{j+1}^* + a_3^* x_j^* - a_4^*(j+1) y_{j+1}^* \right\} \tag{3.18}$$

$$y_{j+2}^* = -\frac{1}{a_5^*(j+1)(j+2)} \left[a_6^* y_j^* + a_4^*(j+1) x_{j+1}^* \right] \tag{3.19}$$

The four independent constants x_0^*, x_1^*, y_0^*, and y_1^* are determined from the prescribed boundary conditions for the adjoint system. Using the recursive relationships, constants x_j^* and y_j^* for j > 1 can be expressed as functions of x_0^*, x_1^*, y_0^*, and y_1^*. The series expressions for W_{un}^* and $W_{\psi m}^*$ can be re-expressed as:

$$W_{un}^* = X_{x0}^* x_0 + X_{y0}^* y_0 + X_{x1}^* x_1 + X_{y1}^* y_1 \tag{3.20}$$

$$W_{\psi m}^* = Y_{x0}^* x_0 + Y_{y0}^* y_0 + Y_{x1}^* x_1 + Y_{y1}^* y_1 \tag{3.21}$$

where

$$X_{x0}^* = 1 - \frac{a_3^*}{2a_1^*}\zeta^2 + \frac{\left(a_2^* + a_7^*\right)a_3^*}{6a_1^{*2}}\zeta^3 + \frac{1}{24a_1^{*2}}\left[-\frac{\left(2a_2^* + a_7^*\right)\left(a_2^* + a_7^*\right)a_3^*}{a_1^*} + a_3^{*2} + \frac{a_3^{*2}a_4^{*2}}{a_5^*}\right]\zeta^4 + \ldots$$

$$X_{y0}^* = -\frac{a_4^* a_6^*}{6a_1^* a_5^*}\zeta^3 + \frac{\left(2a_2^* + a_7^*\right)a_4^* a_6^*}{24a_1^{*2}a_5^*}\zeta^4 + \ldots$$

$$X_{x1}^* = \zeta - \frac{a_7^*}{2a_1^*}\zeta^2 - \frac{-\left(a_2^* + a_7^*\right)a_7^* + a_1^* a_3^* + a_1^* a_4^{*2}/a_5^*}{6a_1^{*2}}\zeta^3 + \frac{1}{12a_1^*}\left\{\left(6a_2^* + 3a_7^*\right) + \frac{1}{6a_1^*}\left[-\frac{\left(a_2^* + a_7^*\right)a_7^*}{a_1^*} + a_3^* + \frac{a_4^{*2}}{a_5^*}\right] + \frac{a_3^* a_7^*}{2a_1^*} + \frac{a_4^{*2}a_7^*}{2a_1^* a_5^*}\right\}\zeta^4 + \ldots$$

$$X_{y1}^* = \frac{a_4^*}{2a_1^*}\zeta^2 - \frac{\left(a_2^* + a_7^*\right)a_4^*}{6a_1^{*2}}\zeta^3 - \frac{1}{12a_1^*}\left[\frac{-\left(2a_2^* + a_7^*\right)\left(a_2^* + a_7^*\right)a_4^*}{2a_1^{*2}} + \frac{a_3^* a_4^*}{2a_1^*} + \frac{a_4^*\left(a_6^* + a_4^{*2}/a_1^*\right)}{2a_5^*}\right]\zeta^4 + \ldots$$

$$Y_{x0}^* = \frac{a_3^* a_4^*}{6a_1^* a_5^*}\zeta^3 - \frac{a_3^* a_4^*\left(a_2^* + a_7^*\right)}{24a_1^{*2}a_5^*}\zeta^4 + \ldots$$

$$Y_{y0}^* = 1 - \frac{a_6^*}{2a_5^*}\zeta^2 + \frac{a_6^* + a_4^{*2}a_6^*/a_1^*}{24a_5^{*2}}\zeta^4 + \ldots \tag{3.22}$$

$$Y_{x1}^* = -\frac{a_4^*}{2a_5^*}\zeta^2 + \frac{a_4^* a_7^*}{6a_1^* a_5^*}\zeta^3 + \frac{1}{24a_5^*}\left\{\frac{a_4^* a_6^*}{a_5^*} + \frac{a_4^*}{a_1^*}\left[-\frac{\left(a_2^* + a_7^*\right)a_7^*}{a_1^*} + a_3^* + \frac{a_4^{*2}}{a_5^*}\right]\right\}\zeta^4 + \ldots$$

$$Y_{y1}^* = \zeta - \frac{a_1^* a_6^* + a_4^{*2}}{6a_1^* a_5^*}\zeta^3 + \frac{a_4^{*2}\left(a_2^* + a_7^*\right)}{24a_1^{*2}a_5^*}\zeta^4 + \ldots$$

Imposing the boundary conditions for the adjoint system on (3.20) and (3.21) yields the frequency equation for λ_{n}^{*}., and the corresponding eigenvectors W_{un}^{*} and $W_{\psi m}^{*}$. The following sections detail the adjoint system boundary conditions, frequency equation, and eigenvectors for four boundary condition cases: hinged-hinged, clamped-free, clamped-clamped, and clamped-hinged.

Hinged-Hinged

The boundary conditions of the adjoint system are

$$W_{un}^{*}(0) = 0 \qquad W_{un}^{*}(1) = 0$$
$$W_{\psi m}^{\prime *}(0) = 0 \qquad W_{\psi m}^{\prime *}(1) = 0$$

The frequency equation is determined to be:

$$X_{y0}^{*}(1)Y_{x1}^{\prime *}(1) - X_{x1}^{*}(1)Y_{y0}^{\prime *}(1) = 0$$

The eigenvectors are defined by:

$$W_{un}^{*} = X_{y0}^{*} - \frac{Y_{y0}^{\prime *}(1)}{Y_{x1}^{\prime *}(1)} X_{x1}^{*}$$

$$W_{\psi m}^{*} = Y_{y0}^{*} - \frac{Y_{y0}^{\prime *}(1)}{Y_{x1}^{\prime *}(1)} Y_{x1}^{*}$$

Clamped-Free

The boundary conditions of the adjoint system are

$$W_{un}^{*}(0) = 0 \qquad W_{\psi m}^{\prime *}(1) = 0$$
$$W_{\psi n}^{*}(0) = 0 \qquad W_{\psi m}^{*}(1) - \frac{1}{l} W_{un}^{\prime *}(1) - \frac{q}{\kappa \hat{A} G} W_{un}^{*}(1) = 0$$

The frequency equation is determined to be:

$$Y_{x1}'^{*}(1)\left[\frac{1}{l}X_{y1}'^{*}(1)-Y_{y1}^{*}(1)+\frac{q}{\kappa AG}X_{y1}^{*}(1)\right]-Y_{y1}'^{*}(1)\left[\frac{1}{l}X_{x1}'^{*}(1)-Y_{x1}^{*}(1)+\frac{q}{\kappa AG}X_{x1}^{*}(1)\right]=0$$

The eigenvectors are defined by:

$$W_{un}^{*}=X_{x1}^{*}-\frac{Y_{x1}'^{*}(1)}{Y_{y1}'^{*}(1)}X_{y1}^{*}$$

$$W_{\psi n}^{*}=Y_{x1}^{*}-\frac{Y_{x1}'^{*}(1)}{Y_{y1}'^{*}(1)}Y_{y1}^{*}$$

Clamped-Clamped

The boundary conditions of the adjoint system are

$$W_{un}^{*}(0)=0 \qquad W_{un}^{*}(1)=0$$
$$W_{\psi n}^{*}(0)=0 \qquad W_{\psi n}^{*}(1)=0$$

The frequency equation is determined to be:

$$X_{x1}^{*}(1)Y_{y1}^{*}(1)-X_{y1}^{*}(1)Y_{x1}^{*}(1)=0$$

The eigenvectors are defined by:

$$W_{un}^{*}=X_{x1}^{*}-\frac{X_{x1}^{*}(1)}{X_{y1}^{*}(1)}X_{y1}^{*}$$

$$W_{\psi n}^{*}=Y_{x1}^{*}-\frac{X_{x1}^{*}(1)}{X_{y1}^{*}(1)}Y_{y1}^{*}$$

Clamped-Hinged

The boundary conditions of the adjoint system are

$$W_{un}^{*}(0)=0 \qquad W_{un}^{*}(1)=0$$
$$W_{\psi n}^{*}(0)=0 \qquad W_{\psi n}'^{*}(1)=0$$

The frequency equation is determined to be:

$$X_{x1}^{*}(1)Y_{y1}'^{*}(1) - X_{y1}^{*}(1)Y_{x1}'^{*}(1) = 0$$

The eigenvectors are defined by:

$$W_{un}^{*} = X_{x1}^{*} - \frac{X_{x1}^{*}(1)}{X_{y1}^{*}(1)} X_{y1}^{*}$$

$$W_{\psi m}^{*} = Y_{x1}^{*} - \frac{X_{x1}^{*}(1)}{X_{y1}^{*}(1)} Y_{y1}^{*}$$

Response Determination

Having determined the eigenpairs for the adjoint system the response calculations can be completed. The response is based upon a modal expansion of the following form:

$$\{w\} = \sum_{m=-\infty}^{+\infty} \{W\}_m q_m \tag{3.23}$$

where q_m are the generalized coordinates. Substituting (3.23) into the equations of motion in matrix form:

$$[M]\{\dot{w}\} = [K]\{w\} + \{P\}$$

Taking the inner product with $\{W^{*}\}_n$, invoking the biorthonormality conditions, the following system of decoupled first order differential equations occur:

$$\dot{q}_m = \lambda_m q_m + Q_m, \qquad m = \pm 1, \pm 2, \ldots \tag{3.24}$$

where

$$Q_m = \left\langle \{P\}^T, \{W^{*}\}_m \right\rangle$$

Recall from Chapter 2, $\{P\}$ is a state vector defined by equation (2.9). Assuming that p is an exponentially decreasing transverse load of the following form

$$p = w\, e^{-i\beta\tau}$$

Substituting into equation (2.9) and evaluating Q_m yields,

$$Q_m = \frac{wc}{\rho I} e^{i\beta\tau},$$

where $$c = \int_0^1 W_{\psi m} d\zeta$$

For zero initial conditions, the solution of (3.24) is the Duhamel integral.

$$q_m = \int_0^t Q_m(\tau) e^{\lambda_m (t-\tau)} d\tau \tag{3.25}$$

Substituting for Q_m yields,

$$q_m = \frac{wc}{\rho I (i\beta - \lambda_m)} \left(e^{i\beta\tau} - e^{\lambda_m \tau} \right) \tag{3.26}$$

The solution contains a homogeneous solution and a particular solution, the particular solution being (3.26). The homogeneous solution is determined from,

$$\dot{q}_m = \lambda_m q_m$$

and therefore,

$$q_m = C e^{\lambda_m \tau}$$

For $\tau = 0$

$$q_m(0) = C$$

Hence, the homogeneous solution is

$$q_m = q_m(0) e^{\lambda_m \tau}$$

The system response u is then calculated using the definition of the state vector $\{w\}$ (2.6) and (3.23):

$$u = \sum_{m=-\infty}^{\infty} W_{um} q_m \tag{3.27}$$

where, when transformed back to real time, we get:

$$q_m = q_m(0)e^{i\lambda_m t} + \frac{wc}{M_m^* \rho I(i\beta - \lambda_m)}\left(e^{-\beta t} - e^{i\lambda_m t}\right)$$

Numerical Analysis and Discussion

The basic data employed in the response calculations is summarized as follows:

$$E = 207 \text{ GPa} \qquad \rho = 7700 \ \frac{\text{kg}}{\text{m}^3} \qquad l = 1.0 \text{ m}$$
$$G = 77.6 \text{ GPa} \qquad \kappa = 0.9$$

The following non-dimensional parameters are used:

$\overline{\Omega} = \Omega / \omega_{10}$ - non-dimensional rotational speed
$\overline{q} = q / q_c$ - non-dimensional follower force
$\beta = \pi r_0 / l$ - Rayleigh beam coefficient

where ω_{10} is the first at-rest natural frequency, q_c is the critical follower force beyond which the system loses its stability based on the Euler-Bernoulli beam theory, and r_0 is the radius of gyration of a circular cross section. The Rayleigh beam coefficient is a reflection of the stubbiness of the beam; as β increases the beam becomes more stubby.

Each beam is subjected to an applied transverse distributed load of the following form:

$$p(\zeta, t) = De^{-\gamma t} \tag{3.28}$$

where D = 10 kN/m and γ = 1 s^{-1}. An Euler-Bernoulli model is used to define the initial deflection at t = 0 sec. of the beam due to the applied transverse distributed load. The initial deflection is defined by the following equation:

$$\frac{EI}{l^4} U(\zeta,0)^{iv} + \frac{q}{l}(1-\zeta)U(\zeta,0)'' = D \tag{3.29}$$

The initial bending deflection $\psi(\zeta,0)$ is found by taking the first derivative of $U(\zeta,0)$.

Clamped-Free Beam

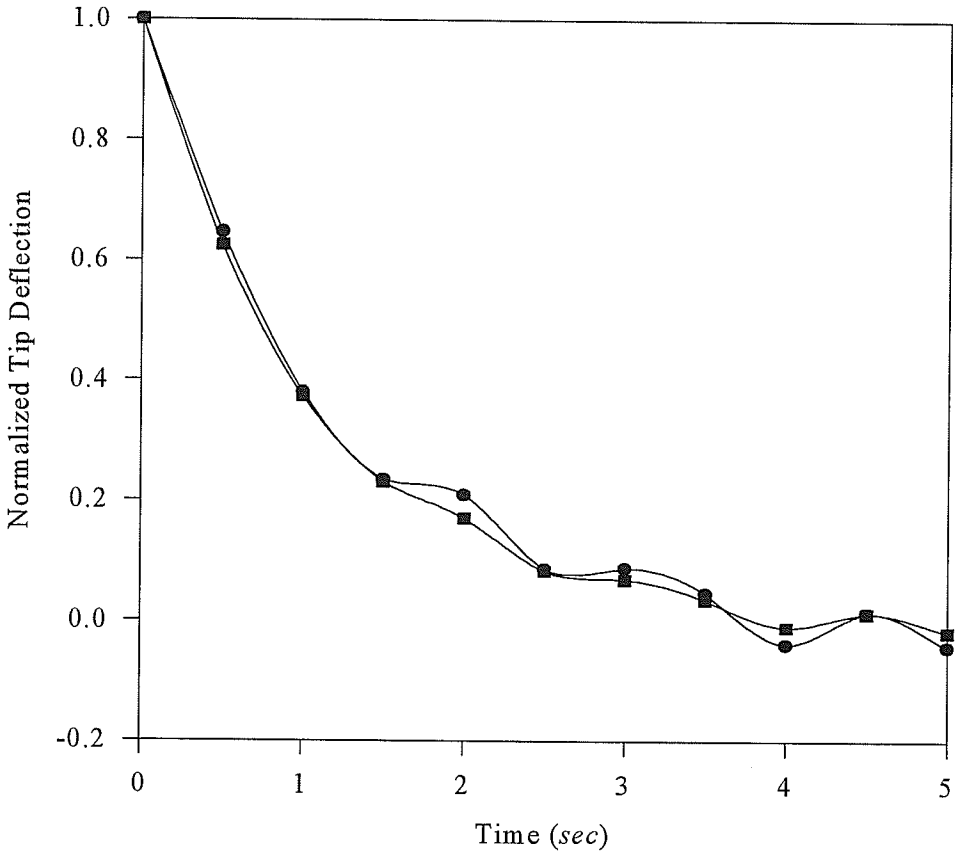

Figure 3.1: Normalized Tip Deflections for Clamped-Free Beams with q=25% (—●— Current Work, —■— Han and Zu (1995))

Figure 3.1 gives the tip deflection of the clamped-free beam as it develops with time for the current work and the work done by Han and Zu (1995). This figure shows good agreement between the forced response of the current work and the forced response calculations done by Han and Zu. Some differences are apparent between the tip deflections. The current work shows more oscillatory behaviour than their work. This is likely because more terms were used to approximate the mode shapes of the real and

adjoint systems than was used by them. This would have the effect of increasing the higher-order contributions to the forced response.

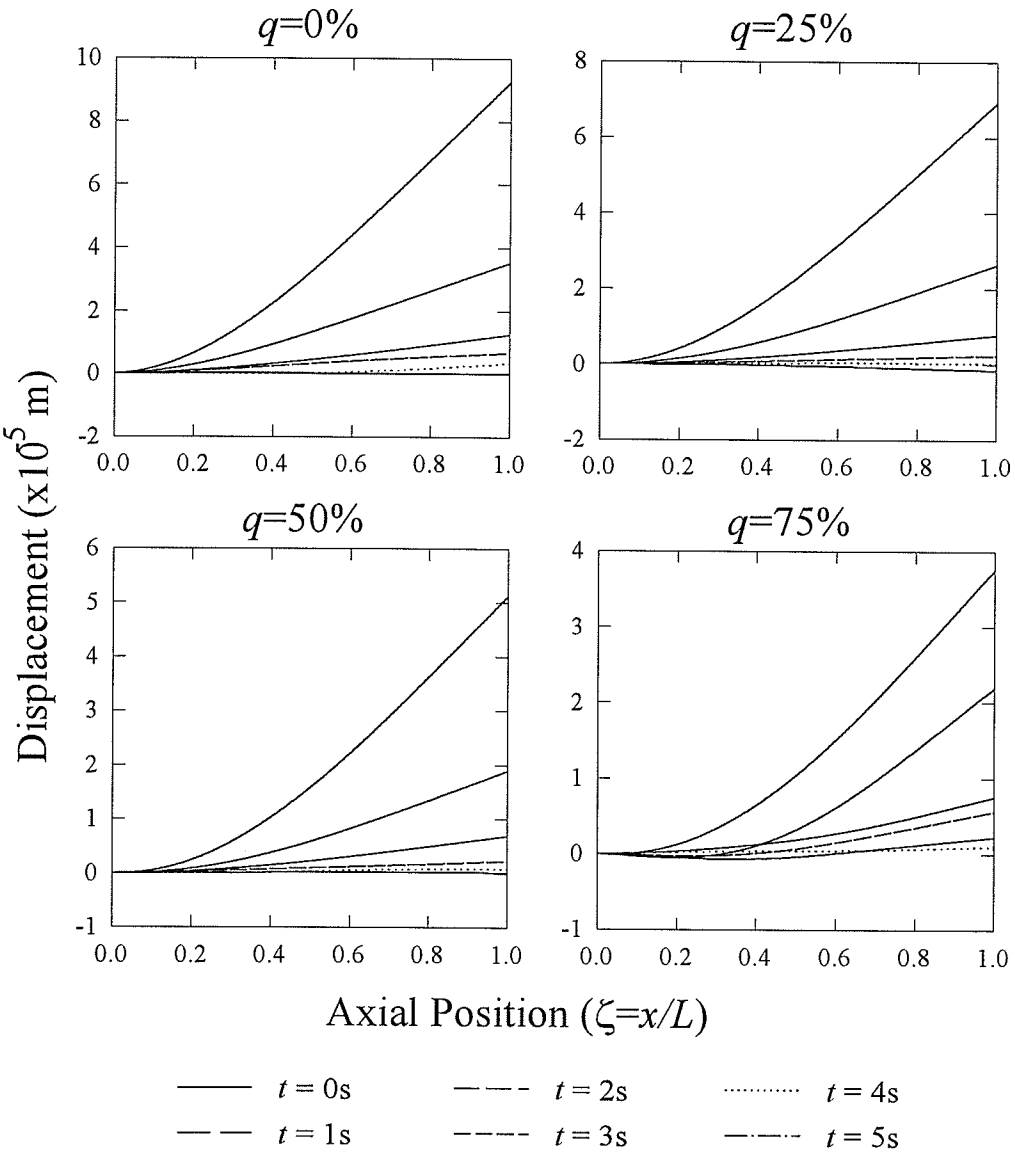

Figure 3.2: Primary Deflections of Clamped-Free Beams

Figure 3.2 shows the primary (in-plane) deflection of the clamped-free beam. It can be seen that the primary deflection decays rapidly with time. The maximum deflection occurs at time $t = 0$ sec. This is expected since the applied transverse load is an exponentially decaying function of time.

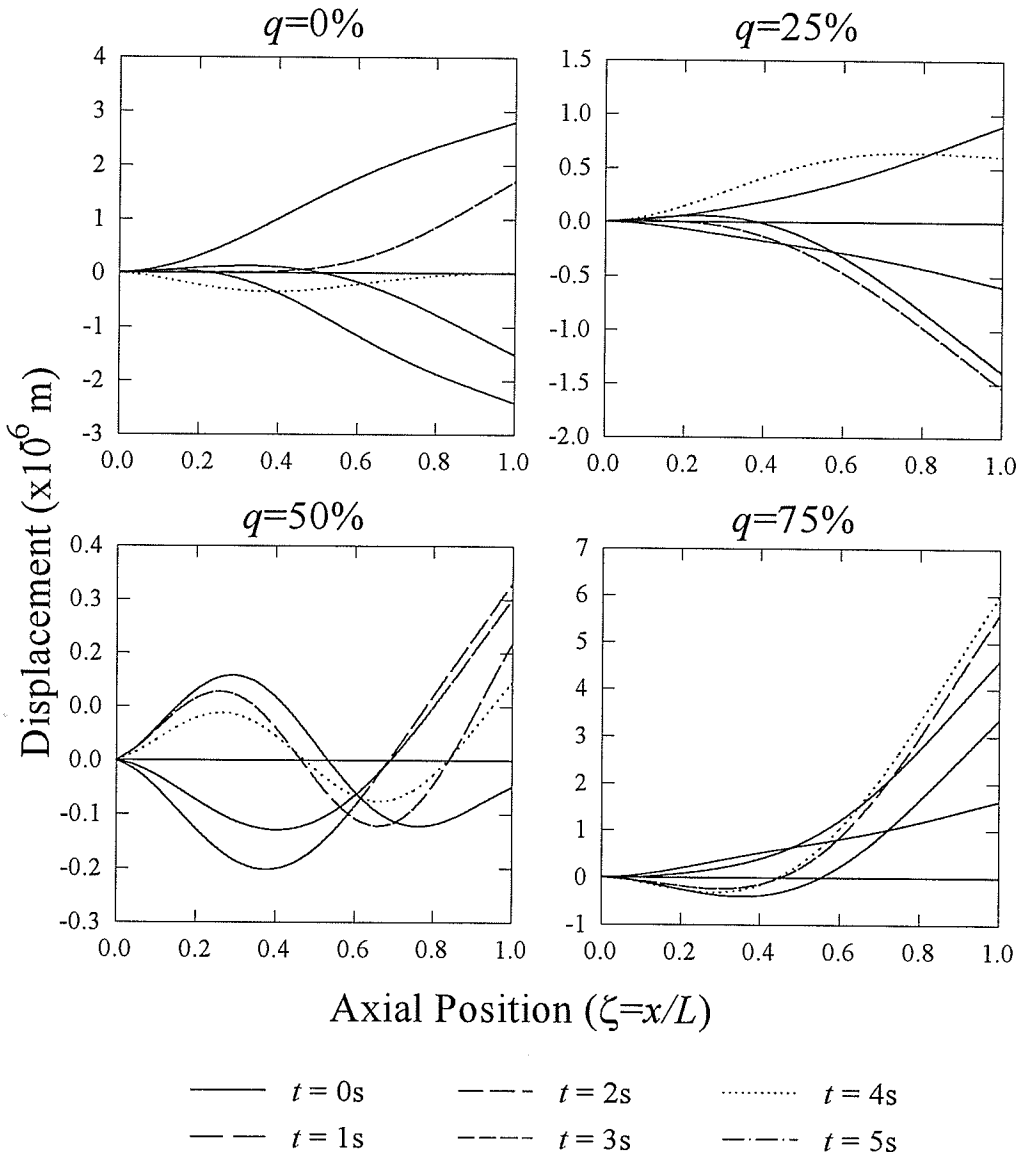

Figure 3.3: Secondary Deflections of Clamped-Free Beams

Figure 3.3 depicts the secondary (out-of-plane) deflections of the clamped-free beam. Observe that these deflections do not decay, but instead oscillate with time. This is due to the fact that the secondary deflections are out of plane with the applied transverse load and therefore, are not affected to the same extent as the primary deflection to changes in the applied transverse load. It should also be noted that the secondary deflections are an order of magnitude less than the primary deflections.

Hinged-Hinged Beam

Figures 3.4 and 3.5 gives the forced vibration response of the hinged-hinged spinning Timoshenko beam with distributed follower forces. Figure 3.4 shows the primary deflections decaying exponentially as the applied transverse load decays.

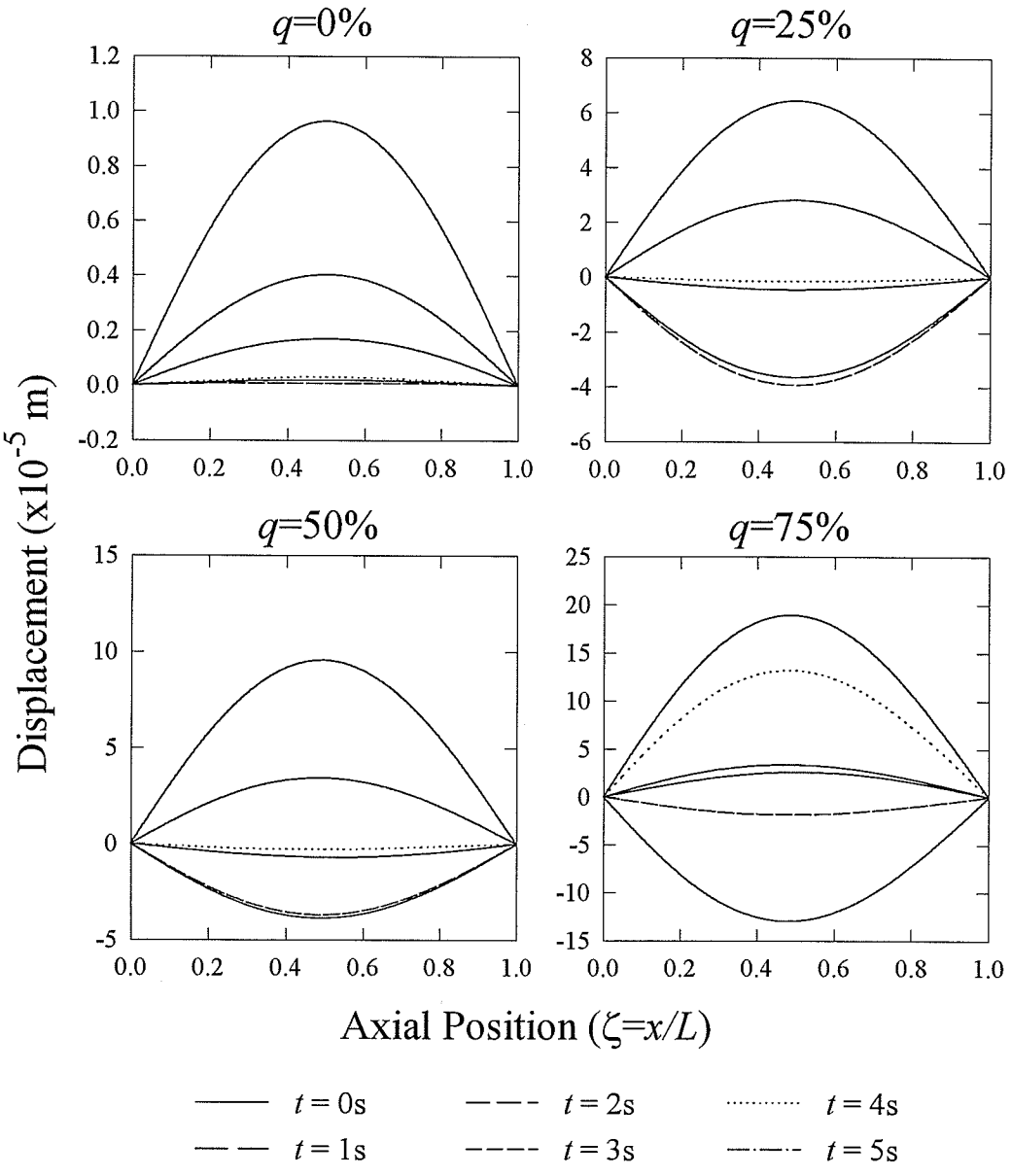

Figure 3.4: Primary Deflections of Hinged-Hinged Beams

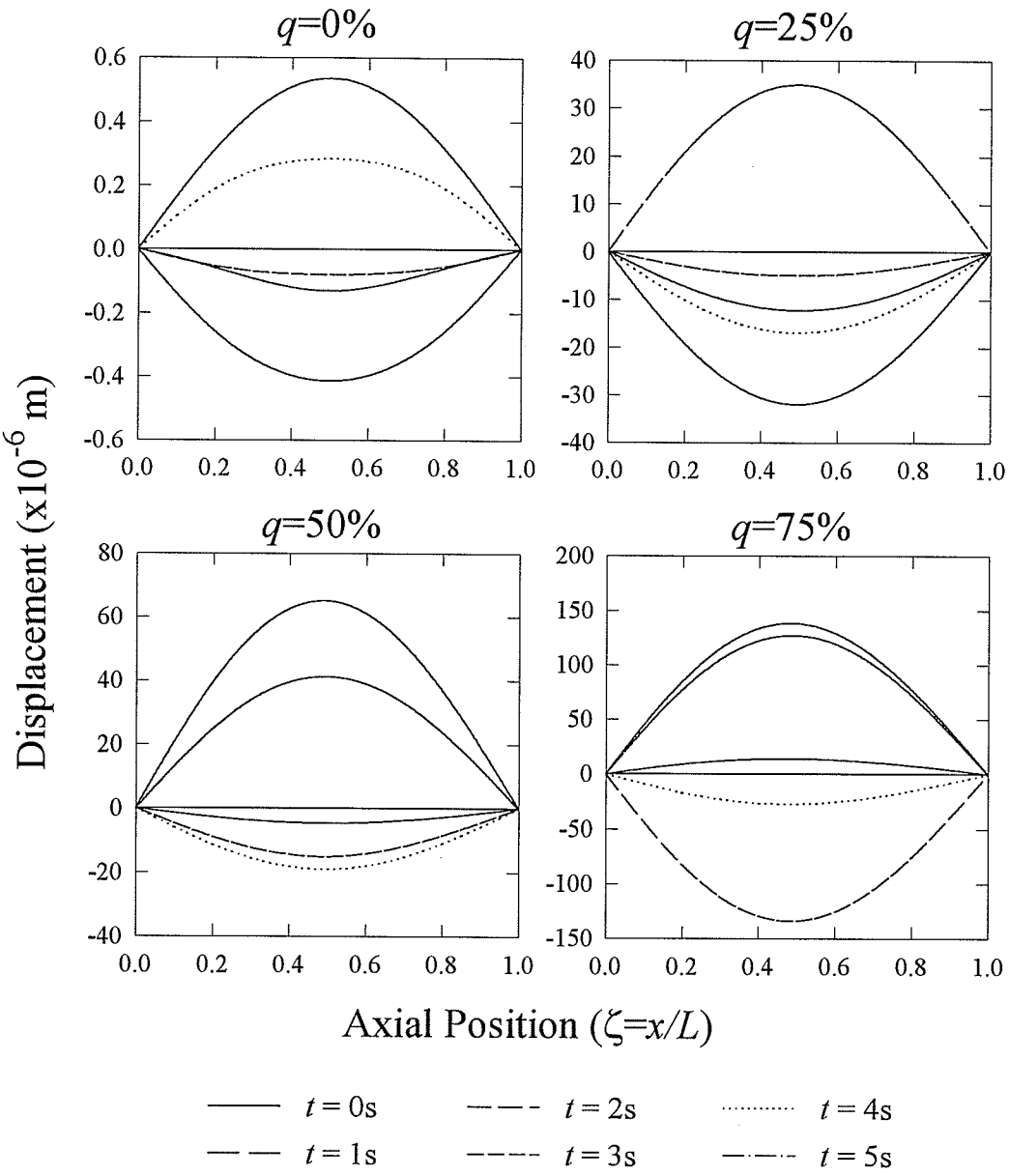

Figure 3.5: Secondary Deflections of Hinged-Hinged Beams

Figure 3.5 shows the independence of the secondary deflections from the decay of the applied transverse load. As with the clamped-free beam the secondary deflections are an order of magnitude less than the primary deflections.

Clamped-Clamped Beam

Figures 3.6 and 3.7 demonstrate the forced response of the clamped-clamped spinning Timoshenko beam with distributed follower forces. Figure 3.6 shows the primary deflections decaying exponentially as the applied transverse load decreases.

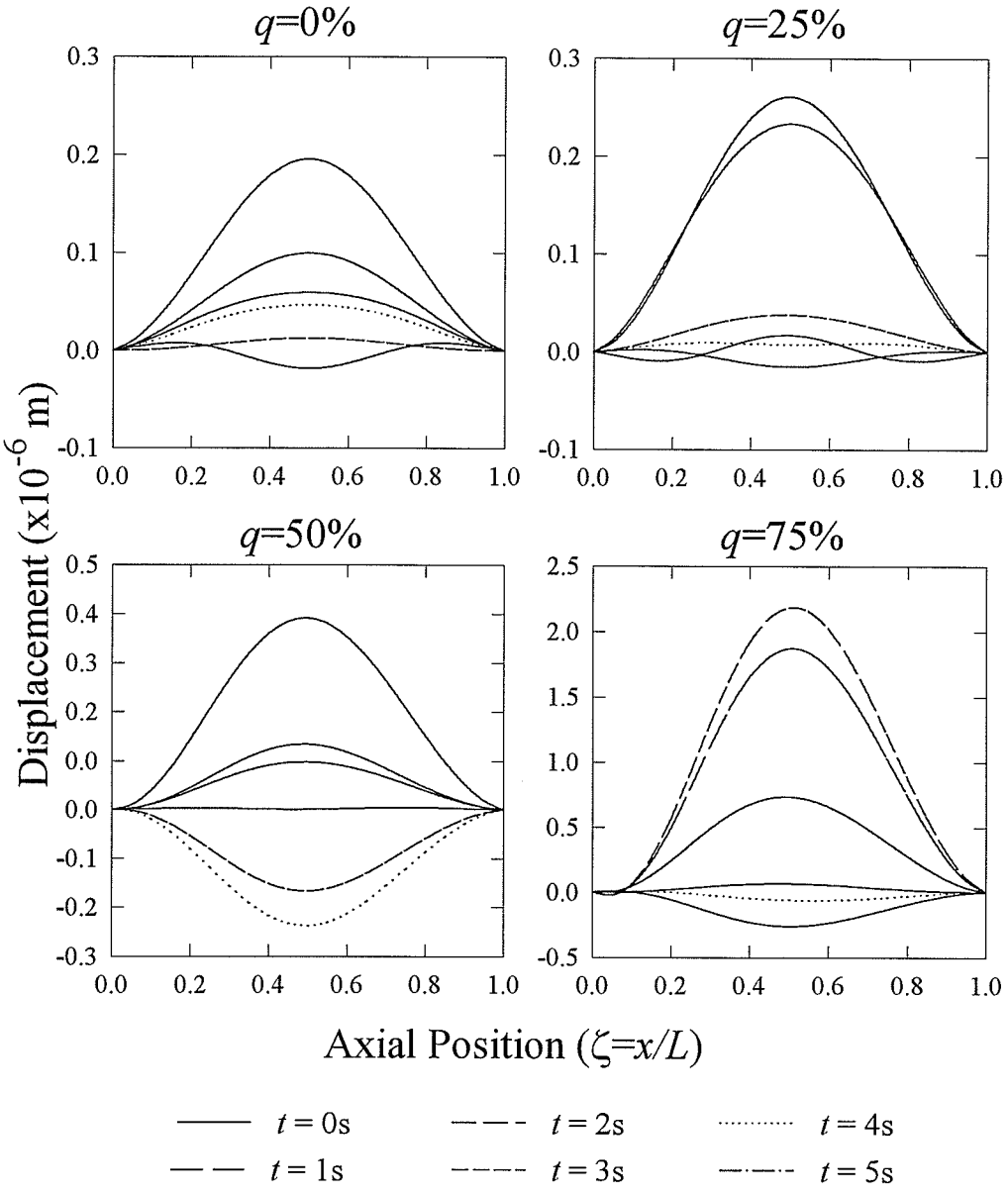

Figure 3.6: Primary Deflections of Clamped-Clamped Beams

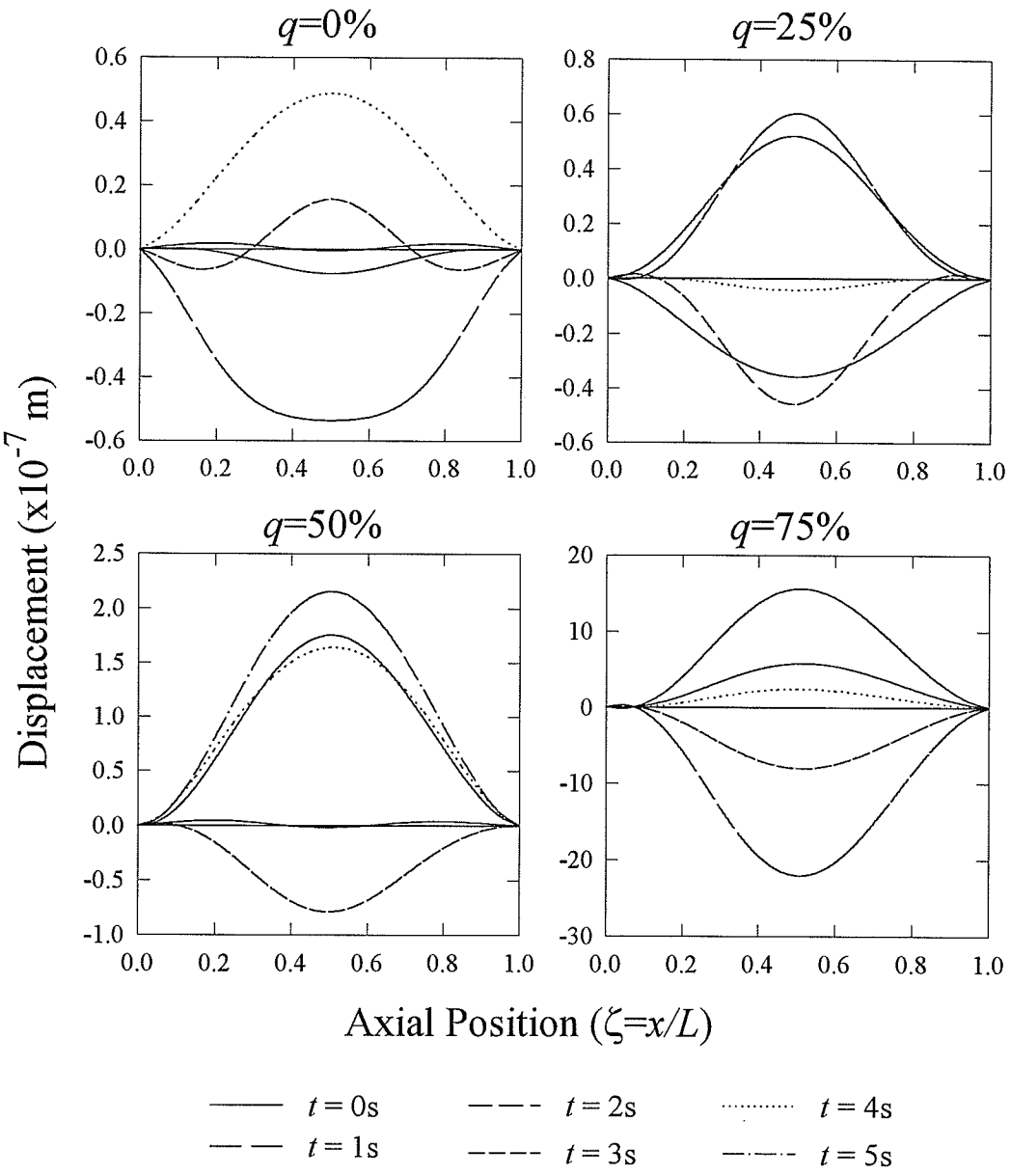

Figure 3.7: Secondary Deflections of Clamped-Clamped Beams

Figure 3.7 shows the oscillatory behaviour of the secondary deflection of the clamped-clamped beam. The secondary deflections are an order of magnitude less than the primary deflections

Clamped-Hinged Beam

Figures 3.8 and 3.9 demonstrate the forced vibration response of the clamped-hinged Timoshenko beam under the influence of distributed follower forces and applied transverse loading. Exponential decay of the primary deflections is seen in Figure 3.8 with increasing time.

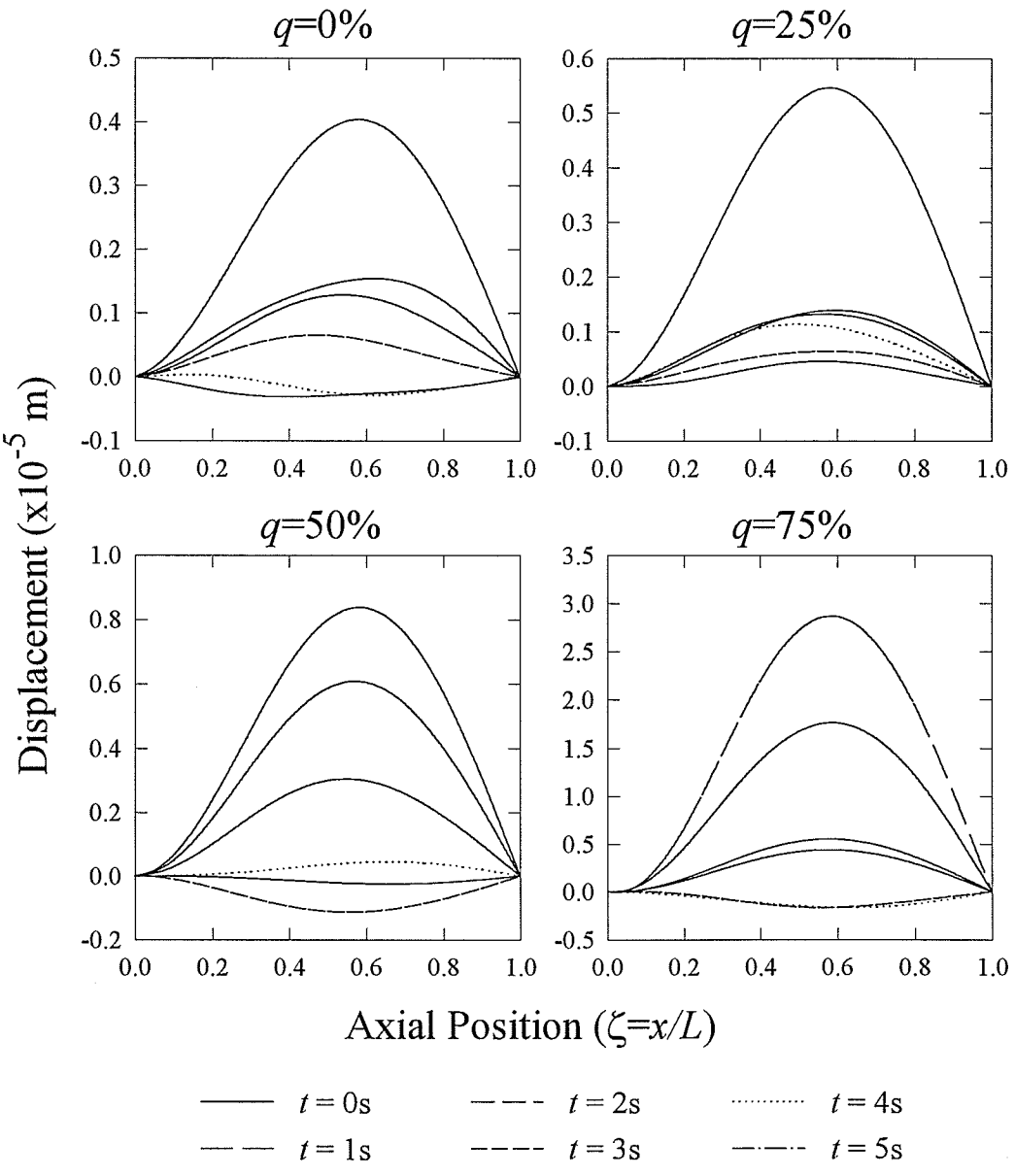

Figure 3.8: Primary Deflections of Clamped-Hinged Beams

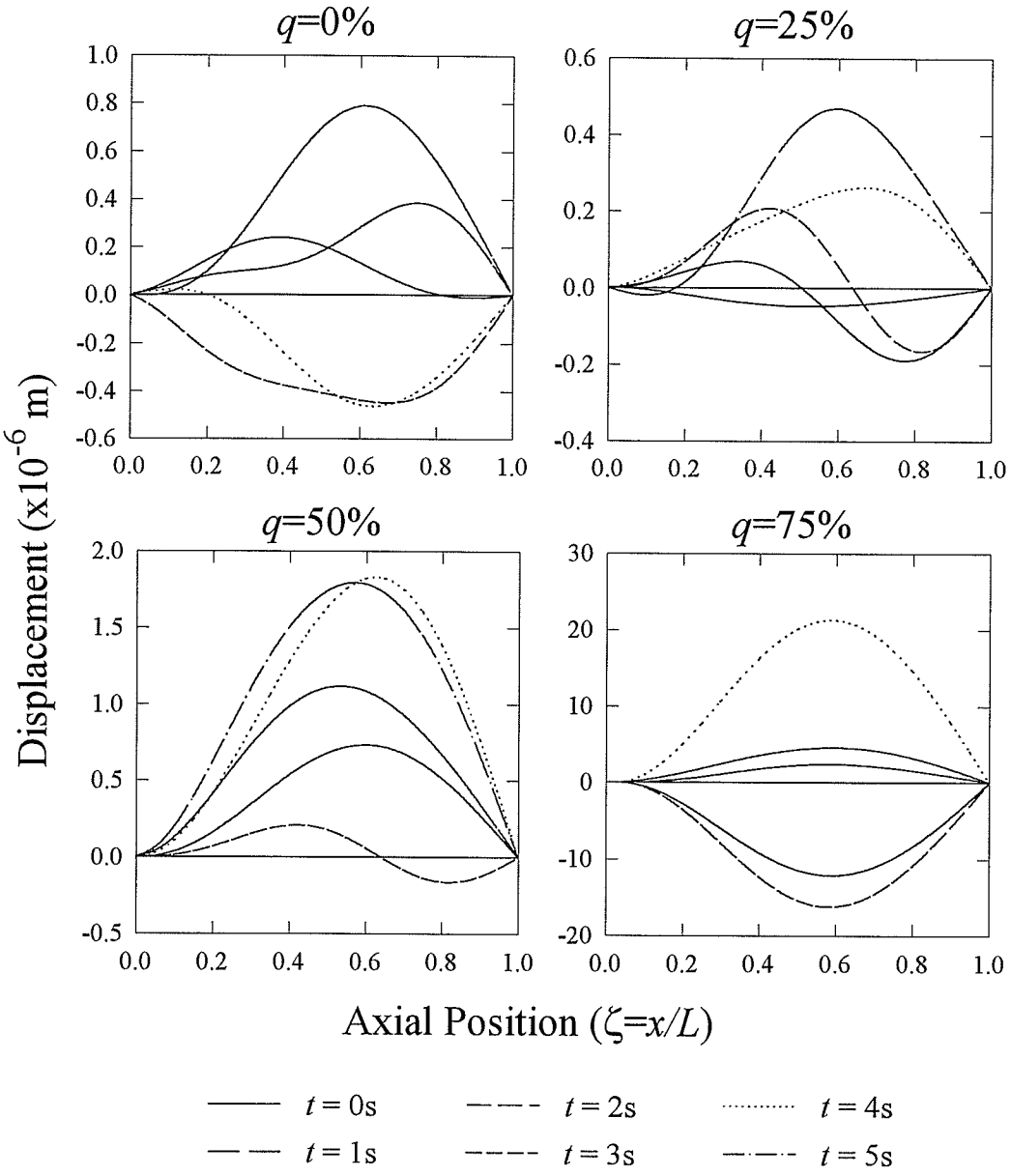

Figure 3.9: Secondary Deflections of Clamped-Hinged Beams

Figure 3.9 shows the oscillatory behaviour of the secondary deflections. As before, the secondary deflections are an order of magnitude less than the primary deflections.

Chapter 4

Summary, Conclusions, and Future Work

Summary

The purpose of this thesis was to apply analytical techniques to the study of the dynamics of non-conservative, spinning Timoshenko beams. Six general boundary condition cases were investigated in Chapter 2 for the free vibration characteristics. Four general boundary condition cases were investigated in Chapter 3 for the forced response to an exponentially decaying applied transverse load.

The free vibration analysis was achieved by applying a differential matrix operator and appropriate state vector definition to reduce the partial differential equations to ordinary differential equations. The resulting system of ordinary differential equations was solved using a series solution. The solution technique is unique in the fact that it requires a PC-based symbolic manipulation package in order to evaluate the frequency equations. Adjoint analysis was required to determine the forced vibration response of the non-conservative beam systems investigated. Once having evaluated the adjoint eigenproblem, modal-expansion methods are applied to the differential matrix operators to solve for the dynamic response.

The free vibration analysis consisted of evaluating each of six boundary condition cases for the natural frequencies and mode shapes. Results were presented demonstrating the variation of the eigenvalues with beam axial spin rate and distributed follower force. Both the forward and backward precession frequencies of the beams were investigated. In

the forced vibration analysis, each of the four boundary condition problems is evaluated for the dynamic response due to a time-varying applied transverse load. The results presented demonstrate the time evolution of the primary and secondary deflections of each beam.

My contributions to the field of spinning beam dynamics has been to apply analytical techniques to handle boundary conditions that were not previously solved using analytical methods. Both free and forced vibrations were investigated in this work.

Conclusions

Conclusions made from the work done in the thesis are as follows.

1. The analytical technique first applied to the solution of the dynamics of a clamped-free spinning Timoshenko beam with non-conservative forces can be extended to more general boundary conditions. A series-type solution can be used to solve the eigenvalue problem for any boundary condition of the following type: clamped, hinged, and free.

2. Clamped-free boundary conditions are the only boundary conditions which experience beam stiffening due to increased follower force load. The other five boundary condition cases show the beam structurally softening as the follower force load increased.

3. The clamped-free and the free-free beams are the only beams which experienced a flutter-type instability as the critical follower force was approached. The other four boundary conditions experience a divergence-type instability as the critical follower force is approached.

4. Critical follower force loads predicted using the Timoshenko beam model are less than the critical follower loads predicted by Euler-Bernoulli beam model.

5. An asymptotic relationship was observed for the backward precession frequencies at increased spin rate for the free-free boundary condition case.

6. A comparison of analytical techniques for spinning Timoshenko beams with zero follower forces show nearly identical predictions for natural frequencies. Slight differences can be attributed to approximations used in the numerical solutions used for each analytical technique.

7. Forced response of the beams showed an exponential decrease with time in the primary deflections corresponding to the exponential decrease in the applied transverse load.

8. Secondary deflections, i.e. out-of-plane deflections, for the forced response of the beams showed an oscillatory behaviour.

9. In all cases, the secondary deflection for the forced vibration response are an order of magnitude less than the primary deflections.

Future Work

There are several possible areas of future work in the study of non-conservative dynamics of spinning Timoshenko beams.

1. A thorough investigation of the stability of non-conservative, spinning Timoshenko beams should be done. This thesis only briefly investigated instability limits for spinning Timoshenko beams with distributed follower forces.

2. A study of the dynamics of spinning Timoshenko beams with both distributed and concentrated follower forces for general boundary conditions should be done.

3. Equations of motion for spinning Timoshenko beams undergoing rigid-body motion and influenced by non-conservative forces should be derived. These equations could be general equations of motion for spinning beam problems, i.e. they would apply to beams with or without rigid-body motion, and with or without non-conservative forces.

4. The spinning Timoshenko beam problem could be expanded to include damping effects in the dynamics of the problem. This would likely result in the equations of motion needing to be rederived and the solution process reinvestigated to solve for the free and forced vibrations of the Timoshenko beam.

Bibliography

Afagh, F. F. and Leipholz, H. H. E., 1990, "Dynamic Response of Elastic Rods Subjected to Uniformly Distributed, Tangential Follower Forces," Ingenieur-Archiv, Vol. 60, pp. 165-175.

Afagh, F.F. and Lee, J.X., 1991, "On the Dynamic Response of Certain Separable and non Self-adjoint Systems," Ingenieur-Archiv, Vol. 60, pp. 422-437.

Bauer, H.F., 1980, "Vibration of a Rotating Uniform Beam, Part I: Orientation in the Axis of Rotation," Journal of Sound and Vibration, Vol. 72, No. 2, pp. 177-189.

Beal, T.R., 1965, "Dynamic Stability of a Flexible Missile under Constant and Pulsating Thrust," AIAA Journal, Vol. 3, No. 3, pp. 486-494.

Bolotin, V.V., 1963, Nonconservative Problems of the Theory of Elastic Stability, Pergamon Press, Oxford, 324 pages.

Chen, Lien-Wen and Ku, Der-Ming, 1994, "Stability of Nonconservatively Elastic Systems Using Eigenvalue Sensitivity," Journal of Vibration and Acoustics, Vol. 116, pp. 168-172.

Craig, Roy R. and Ni, Zhenhau, 1989, "Component Mode Synthesis for Model Order Reduction of Nonclassically Damped Systems," AIAA Journal of Guidance, Dynamics, and Control, Vol. 12, No. 4, pp. 577-584.

Han, Ray P.S. and Zu, Jean W.Z., 1992, "Modal Analysis of Rotating Shafts: A Body-Fixed Axis Formulation Approach", *Journal of Sound & Vibration*, Vol.156, pp. 1-16.

Han, Ray P.S. and Zu, Jean W.Z., 1993, "Analytical Dynamics of a Spinning Timoshenko Beam Subjected to a Moving Load," Journal of the Franklin Institute, Vol. 330, No. 1, pp. 113-129.

Han, Ray P.S. and Zu, Jean W.Z., 1995, "Pseudo Non-Selfadjoint and Non-Selfadjoint Systems in Structural Dynamics," Journal of Sound and Vibration, Vol. 184, pp. 725-743.

Han, Ray P.S. and Zu, Jean W.Z., 1995, "On the Forced Vibrations of a Non-Selfadjoint Spinning Beam Subjected to Follower Forces and Arbitrary Lateral Loads," submitted AIAA Journal.

Huseyin, K., 1978, Vibrations and Stability of Multiple Parameter Systems, Noordhoff International Publishers, Alphen Aan Den Rijn, 216 pages.

Kounadis, A. N., 1980, "On the Derivation of Equations of Motion for a Vibrating Timoshenko Column," Journal of Sound and Vibration, Vol. 73, No. 2, pp. 177-184.

Kounadis, A.N., 1994, "On the Failure of Static Stability Analyses of Nonconservative Systems in Regions of Divergence Instability," International Journal of Solids and Structures, Vol. 31, pp. 2099-2120.

Leipholz, H.H.E. and Madan, Om. P., 1975, "On the Solution of the Stability Problem of Elastic Rods Subjected to Uniformly Distributed, Tangential Follower Forces," Ingenieur-Archiv, Vol. 44, pp. 347-357.

Leipholz, H.H.E., 1983, "On the Fundamental Integrals for Certain Mechanical Problems having Non Self-adjoint Differential Equations," Hadronic Journal, Vol. 6, pp. 1488-1508.

Leung, A.Y.T., 1988, "Dynamic stiffness analysis of follower force," Journal of Sound and Vibration, Vol. 126, pp. 533-543.

Mukhopahyay, M., 1988, "Free Vibration of a Free-Free Beam with Rotary Inertia Effect - A Flexibility Matrix Approach," Journal of Sound and Vibration, Vol. 125, No. 3, pp. 565-569.

Nemat-Nasser S. and Herrmann, G., 1966, "Adjoint Systems in Nonconservative Problems of Elastic Stability," AIAA Journal, Vol. 4, pp. 2221-2222.

Nemat-Nasser, S., 1968, "On Circulatory Force Fields and their Adjoints," ASME Journal of Applied Mechanics, Vol. 90, pp. 829-831.

Park, Y.P. and Mote, C.D. Jr., 1985, "The Maximum Controlled Follower Force on a Free-Free Beam Carrying a Concentrated Mass," Journal of Sound and Vibration, Vol. 98, No. 2, pp. 247-256.

Park, Y.P., 1987, "Dynamic Stability of a Free Timoshenko Beam Under a Controlled Follower Force," Journal of Sound and Vibration, Vol. 113, No. 2, pp. 407-415.

Prasad, S.N. and Herrmann, G., 1969, "The Usefulness of Adjoint System in Solving Nonconservative Stability Problems," International Journal of Solids and Structures, Vol. 5, pp. 727-735.

Platus, D.H., 1992, "Aeroelastic Stability of Slender Spinning Missiles," Journal of Guidance and Control, Vol. 15, No. 1, pp. 144-151.

Rao, B. Nageswara and Rao, G. Venkateswara, 1989, "Large Amplitude Vibrations of Clamped-Free and Free-Free Uniform Beams," Journal of Sound and Vibration, Vol. 134, No. 2, pp. 353-358.

Wu, J.J., 1976a, "On Missile Stability," Journal of Sound and Vibration, Vol. 49, No. 1, pp. 141-147.

Wu, J.J., 1976b, "Missile Stability Using Finite Elements - an Unconstrained Variational Approach," AIAA Journal, Vol. 14, No. 3, pp. 313-319.

Zu, Jean W.Z., and Han, Ray P.S., 1992, "Natural Frequencies and Normal Modes of a Spinning Timoshenko Beam with General Boundary Conditions," Journal of Applied Mechanics.

Zu, Jean W.Z., 1993, Selfadjoint and Non-Selfadjoint Spinning Timoshenko Beam Systems, Ph.D. Dissertation, University of Manitoba, Winnipeg, Manitoba, Canada.

Zu, Jean W.Z., Han, Ray P.S., and Williams, J.J., 1993, "Adjoint Systems Arising from the Non-conservative Problem of Distributed Follower Forces in the Dynamics of Spinning Structures," Department of Mechanical & Industrial Engineering, University of Manitoba.

Zu, Jean W.Z., Han, Ray P.S. and Lu, J., 1994, "On the Precession Frequencies and Critical Speeds of a Spinning Beam", *Fifth Int. Symposium Transport & Dynamics of Rotating Machinery*, ISROMAC-5, Maui.

Appendix A: Nomenclature

A	cross-sectional area
E	Young's modulus
G	shear modulus
I	transverse moment of inertia of circular cross-section
J	polar mass moment of inertia
$[K]$	generalized stiffness matrix
$[K^*]$	adjoint matrix of the generalized stiffness matrix
l	length of the beam
$[M]$	generalized mass matrix
$[M^*]$	adjoint matrix of the generalized mass matrix
$\{P\}$	external load vector in the inertial frame
p	load in the inertial frame
Q_m	generalized force
q	distributed follower force
$\bar{q}$	non-dimensional distributed follower force, q/q_c
q_c	critical distributed follower force
q_m	generalized coordinates
r_0	radius of gyration, $\sqrt{I/A}$
T	kinetic energy
t	time variable
u	complex variable of transverse deflections in the inertial frame
U_e	elastic potential energy
W_U	mode shapes associated with U component
W_ψ	mode shapes associated with ψ component
$\{W\}$	state vector of the inertial frame
$\{W\}_m$	mth eigenvector of the real system

$\{W^*\}_m$	mth eigenvector of the adjoint system
β	Rayleigh beam coefficient, $\pi r_0/l$
δ_{mn}	Kronecker delta function
ζ	non-dimensional length, z/l
κ	shear coefficient
λ	eigenvalues
λ^*	eigenvalues of the adjoint system
ρ	mass density
τ	imaginary time variable
ϕ_X	shear angle in OXZ plane
ϕ_Y	shear angle in OYZ plane
ψ_X	bending angle in OXZ plane
ψ_Y	bending angle in OYZ plane
ψ	complex variable of bending angle in the inertial frame
Ω	spin rate
$\overline{\Omega}$	non-dimensional rotational speed
ω	natural frequency
ω_n	nth natural frequency
ω_{10}	at-rest fundamental natural frequency
$\overline{\omega}$	angular velocity vector

Appendix B: Numerical Analysis Programs

The programs are written using the MapleV programming language. MapleV was used throughout the thesis because of its capabilities for symbolic manipulation. The analytical nature of the thesis determined the requirement to use MapleV. The following set of programs is a representative set of the programs required to generate the data required for each of the six classical boundary conditions. The programs were modified to for each of the six boundary conditions. The following set are the programs used for the fixed-fixed beam free and forced vibration analysis.

Program: fixfix.mpl

```
with(linalg):
Digits:=30:
read `b:fifidata.mpl`:
#
g:=proc(lambda)
a1:=evalf((K*A*G)/(rho*Iner*l)-q[i3]/(rho*Iner*l)):
a2:=evalf(q[i3]/(rho*Iner*l)):
a3:=evalf(lambda^2*A/Iner):
a4:=evalf((K*A*G)/(rho*Iner)):
a5:=evalf(Young/(rho*l^2)):
a6:=evalf(lambda^2-(lambda*Omega[i4]*Jz)/(rho*Iner)-(K*A*G)/(rho*Iner*l)):
#
z:='z':
Xx1:=z:
Xy1:=0:
Yx1:=0:
Yy1:=z:
```

```
#
for n from 0 to N-2 do
    x[n+2]:=(-a2*n*(n+1)*x[n+1]-a3*x[n]+a4*(n+1)*y[n+1])/(a1*(n+1)*(n+2)):
    y[n+2]:=(-a6*y[n]-a4*(n+1)*x[n+1])/(a5*(n+1)*(n+2)):
    XX:=genmatrix([x[n+2]],[x[0],x[1],y[0],y[1]]):
    YY:=genmatrix([y[n+2]],[x[0],x[1],y[0],y[1]]):
    Xx1:=Xx1+XX[1,2]*z^(n+2):
    Xy1:=Xy1+XX[1,4]*z^(n+2):
    Yx1:=Yx1+YY[1,2]*z^(n+2):
    Yy1:=Yy1+YY[1,4]*z^(n+2):
od:
#
z:=1.0:
evalf(Xx1*Yy1-Xy1*Yx1+lambda):
end:
#
writeto(`fixfix.out`):
print(`Free vibration analysis of a fix-fix Timoshenko Beam`):
for i5 from 1 to beta_count do
   print(`////////////////////////////////////////////////////////////`):
   print(`beta = `,beta[i5]):
   writeto(terminal):
   print(`beta = `,beta[i5]):
   appendto(`fixfix.out`):
   r0:=l*beta[i5]/Pi:
   A:=4*Pi*r0^2:
   Iner:=4*Pi*r0^4:
   Jz:=2*rho*Iner:
   f0:=4768.88261:
   alpha:=Young*Iner:
```

```
qb:=80.255*alpha/l^3:
q_count:=4:
q:=array([0.0*qb,0.25*qb,0.5*qb,0.75*qb]):
Omega_count:=3:
Omega:=array([-2.5*f0,0.0*f0,2.5*f0]):
for i4 from 1 by 1 to Omega_count do
  print(`-----------------------------------------------`):
  print(`Omega_bar = `,evalf(Omega[i4]/f0)):
  writeto(terminal):
  print(`Omega_bar = `,evalf(Omega[i4]/f0)):
  appendto(`fixfix.out`):
  for i3 from 1 by 1 to q_count do
    ll:=1:
    writeto(terminal):
    print(`q = `,evalf(q[i3]/qb)):
    appendto(`fixfix.out`):
    for i2 from 1 by 1 to lam_count do
      lambda0:=lam0[i2]:
      i:=1:
      while i<=N0 do
#       writeto(terminal):
#       print(`Iteration step :`,i):
#       print(`lambda0 =`,lambda0):
#       appendto(`fixfix.out`):
        lambda1:=g(lambda0):
        lambda2:=g(lambda1):
        lambda_:=lambda0-((lambda1-lambda0)^2)/
                 (lambda2-2*lambda1+lambda0):
        if abs(lambda_-lambda0) < TOL then
#         print(`Finished`):
```

```
#                print(`lambda = `,lambda_):
                 nd_lambda:=evalf((lambda_^2)*rho*A/alpha):
#                print(`non-dimensional lambda =`,nd_lambda):
                 lam[ll]:=lambda_:
                 ndlam[ll]:=nd_lambda:
                 if (i4=1) and (i3=1) then
                   lam00[ll]:=lambda_:
                 fi:
                 ll:=ll+1:
                 writeto(terminal):
                 print(`lambda =`,lambda_):
                 appendto(`fixfix.out`):
                 break:
               else
                 i:=i+1:
                 lambda0:=lambda_:
               fi:
             od:
             if i>N0 then
               print(`Procedure failed`):
             fi:
           od: #i2
           print(`>>>>>>>  q = `,evalf(q[i3]/qb)):
           for i6 from 1 by 1 to ll-1 do
             print(`lambda =`,lam[i6],ndlam[i6]):
           od:
         od: #i3
       od: #i4
       for i7 from 1 by 1 to ll-1 do
         lam0[i7]:=lam00[i7]:
```

```
    od:
od: #i5
writeto(terminal):
```

Program: fifidata.mpl

```
lam_count:=5:
lam0:=array([1813,4880,9279,14796,21241]):
Young:=2.07*10^11:
mu:=0.3:
rho:=7700.0:
G:=Young/2/(1+mu):
beta_count:=3:
beta:=array([0.05,0.15,0.25]):
l:=1.0:
K:=0.9:
#
N:=50:
TOL:=1.0*10^(-5):
N0:=50:
```

Program: eigen00.mpl

```
Eigenval:=array([
4955.25428,-4579.40565,11883.07445,-10865.02631,20186.05281,-18685.54684]):
Nmode:=6:
```

Program: data00.mpl

```
lambda0:=40000:
Young:=2.07*10^11:
mu:=0.3:
rho:=7700.0:
beta:=0.15:
Omega_bar:=2.5:
l:=1.0:
K:=0.9:
#
r0:=l*beta/Pi:
A:=4*Pi*r0^2:
Iner:=4*Pi*r0^4:
Jz:=2*rho*Iner:
f0:=4768.88261:
alpha:=Young*Iner:
qb:=80.255*alpha/l^3:
G:=Young/2/(1+mu):
q:=0.0*qb:
Omega:=Omega_bar*f0:
N:=50:
TOL:=1.0*10^(-5):
N0:=50:
sw:=10000:
be:=1:
```

Program: uinit.mpl

```
with(linalg);
Digits:=30;
read `b:data.mpl`;
ws:=evalf(sw*l^4/alpha);
qs:=evalf(q*l^3/alpha);
v[0]:=0;
v[1]:=0;
v[4]:=l^4/(4*3*2)*ws;
for i from 1 to 5 do
  v[3*i+4]:=-qs*(3*i+1)*(3*i)/(3*i+4)/(3*i+3)/(3*i+2)/(3*i+1)*v[3*i+1];
  v[3*i+3]:=-qs*(3*i)*(3*i-1)/(3*i+3)/(3*i+2)/(3*i+1)/(3*i)*v[3*i];
  v[3*i+2]:=-qs*(3*i-1)*(3*i-2)/(3*i+2)/(3*i+1)/(3*i)/(3*i-1)*v[3*i-1];
od;
vv:=0;
for j from 0 to 19 do
  vv:=vv+v[j]*(1-z)^j;
od;
vvp:=diff(vv,z);
z:=0;
A:=genmatrix([vv,vvp],[v[2],v[3]],flag);
b:=scalarmul(submatrix(A,1..2,3..3),-1);
A:=delcols(A,3..3);
x:=linsolve(A,b);
v[2]:=x[1,1];
v[3]:=x[2,1];
z:='z';
u0:=vv;
save u0,`uin75.mpl`;
```

Program: intgrt00.mpl

```
read `data00.mpl`:
read `ov251500.m`:
read `av251500.m`:
read `uin00.mpl`:
read `eigen00.mpl`:
#
o0:=diff(u0,z):
NN:=100:
TOL1:=1*10^(-6):
#
aa:=0:
bb:=1:
#
g:=proc(x)
    z:=x:
    if k=1 then
        evalf(Wu[j]*Wus[j]):
    else if k=2 then
        evalf(Wpsi[j]*Wpsis[j]):
    fi: fi:
end:
#
for k from 1 to 2 do
for j from 1 to Nmode do
    APP:=0:
    i:=1:
    TOL_[i]:=10*TOL1:
    a[i]:=aa:
    h[i]:=(bb-aa)/2:
```

```
FA[i]:=g(aa):
FC[i]:=g(aa+h[i]):
FB[i]:=g(bb):
S[i]:=h[i]*(FA[i]+4*FC[i]+FB[i])/3:
L[i]:=1:
while i>0 do
    FD:=g(a[i]+h[i]/2):
    FE:=g(a[i]+3*h[i]/2):
    S1:=h[i]*(FA[i]+4*FD+FC[i])/6:
    S2:=h[i]*(FC[i]+4*FE+FB[i])/6:
    v1:=a[i]:
    v2:=FA[i]:
    v3:=FC[i]:
    v4:=FB[i]:
    v5:=h[i]:
    v6:=TOL_[i]:
    v7:=S[i]:
    v8:=L[i]:
    i:=i-1:
    if abs(S1+S2-v7) < v6 then
        APP:=APP+(S1+S2):
    else
        if v8>=NN then
            print(`Level Exceeded`):
            break:
        else
            i:=i+1:
            a[i]:=v1+v5:
            FA[i]:=v3:
            FC[i]:=FE:
```

```
                FB[i]:=v4:
                h[i]:=v5/2:
                TOL_[i]:=v6/2:
                S[i]:=S2:
                L[i]:=v8+1:
                i:=i+1:
                a[i]:=v1:
                FA[i]:=v2:
                FC[i]:=FD:
                FB[i]:=v3:
                h[i]:=h[i-1]:
                TOL_[i]:=TOL_[i-1]:
                S[i]:=S1:
                L[i]:=L[i-1]:
            fi:
        fi:
    od:
    print(j,APP):
    if k=1 then
    Cu[j]:=APP:
    else if k=2 then
    Co[j]:=APP:
    fi: fi:
od:
od:
save Cu, Co, `intcon00.m`:
```

Program: evect00.mpl

```
with(linalg):
Digits:=30:
read `b:data00.mpl`:
read `b:eigen00.mpl`:
#
for i from 1 to Nmode do
   lambda:=Eigenval[i]:
#
   a1:=evalf((K*A*G)/(rho*Iner*l)-q/(rho*Iner*l)):
   a2:=evalf(q/(rho*Iner*l)):
   a3:=evalf(lambda^2*A/Iner):
   a4:=evalf((K*A*G)/(rho*Iner)):
   a5:=evalf(Young/(rho*l^2)):
   a6:=evalf(lambda^2-(lambda*Omega*Jz)/(rho*Iner)-(K*A*G)/(rho*Iner*l)):
#
   z:='z':
   Xx0:=1:
   Xx0p:=0:
   Xx1:=z:
   Xx1p:=1:
   Xy0:=0:
   Xy0p:=0:
   Xy1:=0:
   Xy1p:=0:
   Yx0:=0:
   Yx0p:=0:
   Yx1:=0:
   Yx1p:=0:
   Yy0:=1:
```

```
  Yy0p:=0:
  Yy1:=z:
  Yy1p:=1:
#
  for n from 0 to N-2 do
    x[n+2]:=(-a2*n*(n+1)*x[n+1]-a3*x[n]+a4*(n+1)*y[n+1])/(a1*(n+1)*(n+2)):
    y[n+2]:=(-a6*y[n]-a4*(n+1)*x[n+1])/(a5*(n+1)*(n+2)):
    XX:=genmatrix([x[n+2]],[x[0],x[1],y[0],y[1]]):
    YY:=genmatrix([y[n+2]],[x[0],x[1],y[0],y[1]]):
    Xx0:=Xx0+XX[1,1]*z^(n+2):
    Xx0p:=Xx0p+diff(XX[1,1]*z^(n+2),z):
    Xx1:=Xx1+XX[1,2]*z^(n+2):
    Xx1p:=Xx1p+diff(XX[1,2]*z^(n+2),z):
    Xy0:=Xy0+XX[1,3]*z^(n+2):
    Xy0p:=Xy0p+diff(XX[1,3]*z^(n+2),z):
    Xy1:=Xy1+XX[1,4]*z^(n+2):
    Xy1p:=Xy1p+diff(XX[1,4]*z^(n+2),z):
    Yx0:=Yx0+YY[1,1]*z^(n+2):
    Yx0p:=Yx0p+diff(YY[1,1]*z^(n+2),z):
    Yx1:=Yx1+YY[1,2]*z^(n+2):
    Yx1p:=Yx1p+diff(YY[1,2]*z^(n+2),z):
    Yy0:=Yy0+YY[1,3]*z^(n+2):
    Yy0p:=Yy0p+diff(YY[1,3]*z^(n+2),z):
    Yy1:=Yy1+YY[1,4]*z^(n+2):
    Yy1p:=Yy1p+diff(YY[1,4]*z^(n+2),z):
  od:
#
  Xy11:=subs(z=1.0, Xy1):
  Xx11:=subs(z=1.0, Xx1):
#
```

```
   Wu[i]:=Xx1-Xy1*Xx11/Xy11:
   Wpsi[i]:=Yx1-Yy1*Xx11/Xy11:
#
od:
save Wu,Wpsi,`ov251500.m`:
#fortran(Wu,filename=`wu_m1.for`):
#fortran(Wpsi,filename=`wpsi_m1.for`):
```

Program: avect00.mpl

```
with(linalg):
Digits:=30:
read `b:data00.mpl`:
read `b:eigen00.mpl`:
#
for i from 1 to Nmode do
   lambda:=Eigenval[i]:
#
   a1:=evalf((K*A*G)/(rho*Iner*l)-q/(rho*Iner*l)):
   a2:=evalf(q/(rho*Iner*l)):
   a3:=evalf(lambda^2*A/Iner):
   a4:=evalf((K*A*G)/(rho*Iner)):
   a5:=evalf(Young/(rho*l^2)):
   a6:=evalf(lambda^2-(lambda*Omega*Jz)/(rho*Iner)-(K*A*G)/(rho*Iner*l)):
   a7:=evalf(2*q/(rho*Iner*l)):
   K2:=evalf(q/(K*A*G)):
#
   z:='z':
   Xx0:=1:
   Xx0p:=0:
   Xx1:=z:
   Xx1p:=1:
   Xy0:=0:
   Xy0p:=0:
   Xy1:=0:
   Xy1p:=0:
   Yx0:=0:
   Yx0p:=0:
   Yx1:=0:
```

```
  Yx1p:=0:
  Yy0:=1:
  Yy0p:=0:
  Yy1:=z:
  Yy1p:=1:
#
  for n from 0 to N-2 do
    x[n+2]:=-((a2*n*(n+1)+a7*(n+1))*x[n+1]+a3*x[n]-a4*(n+1)*y[n+1])/
        (a1*(n+1)*(n+2)):
    y[n+2]:=-(a6*y[n]+a4*(n+1)*x[n+1])/(a5*(n+1)*(n+2)):
    XX:=genmatrix([x[n+2]],[x[0],x[1],y[0],y[1]]):
    YY:=genmatrix([y[n+2]],[x[0],x[1],y[0],y[1]]):
    Xx0:=Xx0+XX[1,1]*z^(n+2):
    Xx0p:=Xx0p+diff(XX[1,1]*z^(n+2),z):
    Xx1:=Xx1+XX[1,2]*z^(n+2):
    Xx1p:=Xx1p+diff(XX[1,2]*z^(n+2),z):
    Xy0:=Xy0+XX[1,3]*z^(n+2):
    Xy0p:=Xy0p+diff(XX[1,3]*z^(n+2),z):
    Xy1:=Xy1+XX[1,4]*z^(n+2):
    Xy1p:=Xy1p+diff(XX[1,4]*z^(n+2),z):
    Yx0:=Yx0+YY[1,1]*z^(n+2):
    Yx0p:=Yx0p+diff(YY[1,1]*z^(n+2),z):
    Yx1:=Yx1+YY[1,2]*z^(n+2):
    Yx1p:=Yx1p+diff(YY[1,2]*z^(n+2),z):
    Yy0:=Yy0+YY[1,3]*z^(n+2):
    Yy0p:=Yy0p+diff(YY[1,3]*z^(n+2),z):
    Yy1:=Yy1+YY[1,4]*z^(n+2):
    Yy1p:=Yy1p+diff(YY[1,4]*z^(n+2),z):
  od:
#
```

```
   Xx11:=subs(z=1,Xx1):
   Xy11:=subs(z=1,Xy1):
#
   Wus[i]:=Xx1-Xx11/Xy11*Xy1:
   Wpsis[i]:=Yx1-Xx11/Xy11*Yy1:
#
od:
save Wus,Wpsis,`av251500.m`:
#fortran(Wus,`wus_m1.mpl`):
#fortran(Wpsis,`wpsis_m1.mpl`):
```

Program: force00.mpl

```
read `data00.mpl`:
read `ov251500.m`:
read `av251500.m`:
read `eigen00.mpl`:
read `uin00.mpl`:
read `intcon00.m`:
o0:=diff(u0,z):
U:=0.0:
for i from 1 to Nmode do
  print(`q=0%, Nmode =`,i):
  CC_[i]:=evalf(int(Wus[i],z=0..1,continuous));
  Cu_[i]:=Cu[i];
  Co_[i]:=Co[i];
  Du_[i]:=evalf(int(expand(Wus[i]*u0),z=0..1,continuous));
  Do_[i]:=evalf(int(expand(Wpsis[i]*o0),z=0..1,continuous));
  olam:=Eigenval[i]:
  alam:=Eigenval[i]:
  Ms:=evalf((olam+alam)*(A/Iner*Cu_[i]+Co_[i])-Omega*Jz/(rho*Iner)*Co_[i]);
  q0:=evalf((alam*A/Iner*Du_[i]+(alam-Omega*Jz/(rho*Iner))*Do_[i])/Ms);
  q[i]:=q0*exp(olam*T*I)-sw*CC_[i]/(be*I-olam)/(rho*Iner)/Ms*(exp(-be*T) \
      -exp(olam*T*I));
  U:=U+expand(Wu[i]*q[i]):
od:
save CC_,Cu_,Co_,Du_,Do_,U,`u00temp.m`:
Ur:=evalc(Re(U)):
Ui:=evalc(Im(U)):
save Ur,Ui,`uu00t.m`:
```